UCRL-JRNL-205844

LAWRENCE
LIVERMORE
NATIONAL
LABORATORY

Emission Line Spectra of S VII–S XIV in the 20–75 Å wavelength region

J. K. Lepson, P. Beiersdorfer, E. Behar, S. M. Kahn

July 23, 2004

For submission to Astrophysical Journal

Emission line spectra of S VII–S XIV in the 20 – 75 Å wavelength region

J. K. Lepson

Space Sciences Laboratory, University of California, Berkeley, CA 94720

lepson@ssl.berkeley.edu

P. Beiersdorfer

Department of Physics and Advanced Technology, Lawrence Livermore National Laboratory, Livermore, CA 94550

beiersdorfer@llnl.gov

E. Behar

Physics Department, Technion - Israel Institute of Technology, Haifa 32000, Israel

behar@physics.technion.ac.il

and

S. M. Kahn

Physics Department, Stanford University, Stanford, CA 94305, U.S.A.

skahn@slac.stanford.edu

ABSTRACT

As part of a larger project to complete a comprehensive catalogue of astrophysically relevant emission lines in support of new-generation X-ray observatories using the Lawrence Livermore electron beam ion traps EBIT-I and EBIT-II, we present observations of sulfur lines in the soft X-ray and extreme ultraviolet regions. Our database includes wavelength measurements with standard errors, relative intensities, and line assignments for 127 transitions of S VII through S XIV between 20 and 75 Å. The experimental data are complemented with a full set of calculations using the Hebrew University Lawrence Livermore Atomic Code (HULLAC). A comparison of the laboratory data with *Chandra* measurements of Procyon allows us to identify S VII–S XI lines.

Subject headings: line: identification–methods: laboratory, analytical–stars: coronae, stars–Procyon

1. Introduction

Satellite observations in the extreme ultraviolet region provide unique and valuable diagnostic opportunities for astronomers and astrophysicists. The extreme ultraviolet spectral region, which at the short wavelength side overlaps with the soft X-ray region, contains a wealth of emission lines that can be used for determining plasma properties and elemental abundances over a wide temperature range. The region between 20 and 80 Å has received scant attention, however, even in solar measurements. Previous observations by the *Extreme Ultraviolet Explorer* stopped at 70 Å, while crystal spectrometers aboard various missions covered the regions below 20 Å. Because this region has been virtually unstudied, even in the laboratory, the relevant databases are essentially empty. Observations in the soft X-ray region by the *Chandra X-ray Observatory* and *XMM-Newton* are now providing high-resolution measurements, which have far outpaced the databases. There are many more lines in these spectra than can be currently identified, as is graphically illustrated by Chandra spectra of Capella (Brinkman 2000) and Procyon (Raassen et al. 2002).

Line lists for the L-shell emission of all elements aside from iron are highly deficient. (For iron, see Brown et al. 2002) ApJS, 140, 589 and Behar, Cottam, & Kahn 2001), ApJ 548, 966) In the case of sulfur, for example, the MEKAL database (Mewe, Kaastra, & Liedahl 1995a) includes 47 lines for S VII through S XIV between 20 and 75 Å. The CHIANTI database (Dere et al. 1995, 2001) has recently been extended to below 50 Å, and includes 13 lines of S XIV, but only nine lines for the other charge states of sulfur, for a total of 22 lines. However, long-term exposures of stellar coronae have shown a wealth of weak lines. These weak lines raise the "background" level for the brighter, known lines and add uncertainty to their interpretation. Moreover, they obscure the true thermal background level, requiring the assumption of a hotter plasma temperature than otherwise necessary to fit the elevated radiation level (Beiersdorfer et al. 1999b). Contributions to these unidentified lines may come from magnesium, sulfur, argon, calcium, iron, and nickel. Identification of as many ions as possible of a given element provides a measurement of the emission measure (EM) distribution shape, which is independent of assumptions on the chemical composition. In fact, the only reliable method to disentangle the temperature and the chemical structures and to obtain robust, model-independent abundance values is to compare the EM distribution derived from many ions of different elements. To that end, the L-shell ions are a crucial addition to the K-shell lines regularly observed in astrophysical X-ray spectra and the uncertainties associated with the wavelengths and intensities of L-shell lines greatly impede our efforts to fully understand astrophysical X-ray sources. Calculations are helpful to predict emission from these elements. A major problem, however, is that the accuracy of the calculated wavelengths is limited, as the structure of the intermediate ionization stages of all high-Z ions of astrophysical interest are significantly affected by electron-electron interactions, and these ionization stages must be calculated in intermediate coupling. Wavelength errors of a percent are not uncommon, and no *ab initio* code can consistently calculate wavelengths to better than a few tenths of a percent for mid-Z L-shell or M-shell ions. Without knowing the proper line positions, spectral modeling is beset by a host of potential problems. Flux may be assigned to the wrong transitions, ionization stages, or even elements. Lines calculated by any model are likely to be in the wrong place if they are not verified experimentally. An error of just one or two percent in the line positions has a tremendous effect on the predicted flux assignments, which is compounded if it leads to errors in line assignment. Such errors are likely given the great density of lines observed by *Chandra* and *XMM-Newton*.

Laboratory measurements are needed to locate the lines and to correlate them to the proper charge state. We have presented earlier extensive measurements of the L-shell emission spectra of argon (Lepson et al. 2003), following line lists of the iron L-shell emission in the soft X-ray band (Brown et al. 2002) and of the iron M-shell emission in the EUV (Lepson et al. 2002). We present here the L-shell emission spectra (transitions of the type $n\ell' \rightarrow 2\ell$), of the sulfur ions S VII–S XIV in the wavelength range of 20–75 Å. Measurements concentrate on the strongest features in each charge state as these are the ones most likely to be observed in astrophysical plasmas. Our measurements are complemented by a full set of calculations from the Hebrew University – Lawrence Livermore Atomic Code (HULLAC, Bar-Shalom, Klapisch, & Oreg 2001).

2. Spectroscopic measurements

Spectroscopic measurements were taken on the Lawrence Livermore electron beam ion traps EBIT-I and EBIT-II. EBIT-I and EBIT-II are well-suited for such investigations because they can be operated at the low voltages (100–1,000 eV) necessary to produce the charge states we investigated. Moreover, different charge states can be produced simply by changing the voltage of the electron beam. As the voltage increases, higher charge states appear when their ionization potentials are exceeded, and lower charge states decline and disappear as they become ionized. Ideally, charge states appear and disappear one by one as the voltage increases. In practice, there is some mixing because of recombination. Sulfur was introduced into the trap by a gas injection system. During this experiment we used a relatively high gas pressure to emphasize the lines. This continuous source of neutral sulfur resulted in the retention of the lower charge states even at higher beam energies. Consequently, spectra taken at the highest voltages contained all the charge states from S VII through S XIV. By systematically recording spectra at different energies and observing the rise and relative decline of different charge states, however, it is possible to determine which emission lines belong to which charge state.

Spectra were measured on EBIT-II with a grazing-incidence spectrometer (Utter et al. 1999) employing an average 2,400 line/mm flat-field grating developed by Harada & Kita (1980; Nakano et al. 1984) with a 1.3° angle of incidence, and an instrumental resolution of ~ 300 (at 25 Å) to ~ 500 (at 50 Å). Readouts were taken with a back-illuminated, liquid nitrogen-cooled CCD camera with a one inch square array of $1{,}024 \times 1{,}024$ pixels.

Wavelength calibrations were performed periodically throughout the experimental run using the well-known hydrogenic and heliumlike K-shell emission lines of carbon, oxygen, and nitrogen. These lines were observed in first order and provided an accurate calibration region between 19 Å and 40 Å.

For calibration of wavelengths > 40 Å, we used the S VII lines $2p^5_{3/2}3s^3_{1/2}P_1$ (commonly labeled 3G) and $2p^5_{1/2}3s^1P_1$ (commonly labeled 3F) which we calibrated separately, using measurements taken on EBIT-I with a grazing-incidence spectrometer (Beiersdorfer et al. 1999a) employing an average 1,200 line/mm flat-field grating developed by Harada & Kita (1980; Nakano et al. 1984) with a 3° angle of incidence. Readouts were taken with a back-illuminated, liquid nitrogen-cooled CCD camera with a one inch square array of $1{,}024 \times 1{,}024$ pixels. The instrumental resolution is ~ 300 at 100 Å. These spectra were calibrated using the well-known K-shell emission lines of nitrogen, in particular the N VII Lyman-α line and the N VI resonance line commonly referred to as w, as described by Beiersdorfer et al. (1999a). These lines were observed in the 2nd through 6th orders (49–172 Å), and the S VII lines were measured in 1st and 2nd orders.

Spectra were periodically taken without an active trap, i.e., without a potential applied to the trap electrodes. These spectra enabled us to determine the level of background emission (including visible light from the electron-gun filament, to which the CCD camera is sensitive), which was then subtracted from the sulfur spectra to yield background-corrected spectra.

After identification, we measured the relative fluxes of the emission lines for each charge state, and corrected for differing sensitivity of the spectrometer (grating detector) at different wavelengths (Lepson et al. 2001).

3. The spectra

Figure 1 shows representative spectra of sulfur taken on EBIT-II at beam energies of 300, 450, and 750 eV, with the strongest sulfur lines labeled by charge state. Charge states from S VII through S XIV are present. The charge states can be identified by comparing spectra taken at different beam energies: as the beam energy increases, emission lines of higher charge states appear as their ionization thresholds are surpassed. Therefore, each new spectrum contains an additional, higher charge state. We measured at 10 energies between 200 and 750 eV, and additionally at 2 keV. Tables 1–8 present the major features for each charge state, along with our measured wavelengths and relative line strengths (intensity corrected for spectrometer response). The tables also list predicted wavelengths and strengths from our present HULLAC code calculations, as well as the responsible line transition. We include lines from the two most widely used astronomical databases, MEKAL and CHIANTI, where those lines can be compared with the measured lines.

Line wavelengths in the HULLAC code are calculated in intermediate coupling and by means of the relativistic parametric potential method (Klapisch et al. 1977). Line intensities in the present work were calculated in the coronal steady-state approximation assuming that the only important atomic processes within a given ionic state are electron impact excitation and spontaneous radiative decays. The electron energy distribution available for excitation is assumed to be Maxwellian, corresponding to an electron temperature ranging from T_e=600 eV (for S VII – S IX) to T_e=1500 eV(for S XII – S XIV). Calculations assumed a density of $5 \times 10^{11} cm^{-3}$. Given the low densities at which the measurements were taken, line self-absorption in the trap is neglected.

4. Comparison with theory

We also constructed synthetic spectra derived from the HULLAC calculations that we overlaid onto the EBIT-II spectra. We did not adjust the EBIT-II spectra for the detector responsivity in these figures as this enhances unsightly noise in the regions where responsivity is low. Instead, we adjusted the synthetic HULLAC spectra by the detector response so that they are directly comparable with our measurements.

Figures 2–9 show details of spectra from EBIT-II and compare them with the HULLAC calculations, covering all the charge states from S VII through S XIV. We make two representations of synthetic HULLAC spectra. In both cases, the spectra are intensity corrected by the detector response function (see Fig. 1 in Lepson et al. 2003) and are normalized to the strongest EBIT-II peak in each charge state in order to make them directly comparable with the measured spectra. In the first overlay, no adjustments are made for differences in line position; this demonstrates the accuracy of the calculations for line identification. In the second overlay, we correct the position of each HULLAC line so that it coincides with the line as observed with EBIT-II; this is our best effort at adjusting theory to fit the laboratory measurements.

The HULLAC calculations do a reasonable job of reproducing the spectra observed on EBIT-II. In particular, most strong lines are rendered accurately enough to allow ready identification in our relatively simple spectra, which have just a single element, and in which we can distinguish between charge states taken at different beam energies. Yet even in this simplified system, it is often impossible to accurately assign the weaker emission lines: the wavelength accuracy of the calculations (Tables 1–8) is not sufficient to distinguish between the many weak lines, which are much harder to separate by charge state, and which are often clustered closer together than either the accuracy of the calculations or the resolution of the spectrometer. This situation does not change appreciably when performing a calculation for a monoenergetic electron beam, which would more closely match our conditions.

In Table 10 we make a cursory comparison of our laboratory measurements with the two most widely-used databases, MEKAL and CHIANTI, noting the number of lines reported for each charge state investigated here. Both databases do best with the simplest, fewest-electron systems of S XIV, and worse for the more complicated lower charge states, although MEKAL has some lines for all charge states and contains most of the lines we found in neonlike S VII.

Our spectra also contain a line not predicted by calculations. This line corresponds to the $(1s^2 2s_{1/2}^2 2p_{1/2} 2p_{3/2}^4 3s_{1/2})_0 \rightarrow (1s^2 2s_{1/2}^2 2p_{1/2}^2 2p_{3/2}^4)_0$ transition in S VII and is labelled S VII-9 in the figures and in Table 1. This transition is strictly forbidden by selection rules. However, it becomes possible if the ion is embedded in a magnetic field, as described by Beiersdorfer, Scofield, & Osterheld (2003). The S VII line is a spectral diagnostic of magnetic field strength and increases in strength relative to the 3F line (S VII-8) as the magnetic field is increased. The magnetic field in EBIT-I and EBIT-II is 30 kG, and is sufficient to produce the line even in the presence of collisions.

5. Comparison with Procyon

Raassen et al. (2002; their Tables 1 & 2) identified a number of possible lines of S VII through S XIII in the region 20–75 Å in a spectrum of Procyon taken with the *Chandra* low energy transmission grating spectrometer (LETGS). They listed 15 lines from *Chandra* for which sulfur was given as a possible identification in either MEKAL (Kaastra & Mewe 1993; Mewe, Kaastra, & Liedahl 1995), Kelly (1987) or Doschek & Cowan (1984). In some cases, sulfur was just one of several identification possibilities. We compared EBIT-II spectra to the *Chandra* data by overlaying the two. This allows a quick visual confirmation of the presence of each charge state since not only must there be lines in the same locations, but they also must match in relative intensity. From this we identify the presence of S VII through S XI. The presence of S XII and S XIII is doubtful; if they are present they are in very small amounts. We found no evidence of S XIV. In Fig. 10 we show overlays of a spectrum from the *Chandra* LETGS with spectra from EBIT-II for S VII, S VIII, and S IX–S X. The *Chandra* spectra have a higher resolution than the EBIT-II data shown here, but the line clusters are evident. In some cases, blends with other elements in Procyon make the matches less obvious, e.g., the S IX and S X lines at 49.3 Å (Fig. 10c) blend with Ar IX in the *Chandra* spectrum. We have acquired a new spectrometer with resolution comparable to that of *Chandra* (Beiersdorfer et al. 2004), with which we intend to take further measurements, particularly of S X, whose strongest lines lie in the region of the carbon edge and are thus not seen in the present spectra due to a carbon film on the detector.

The spectrum of S VII merits further discussion as there is a discrepancy between our measurements and *Chandra* observations. The 3s $\rightarrow$ 2p line at 72.9 Å, labeled VII-10 in Table 1 (commonly referrred to as 3G), is much stronger compared to its companion at 72.7 Å, labelled VII-11 (commonly referred to as 3H or M2), in the *Chandra* spectrum than in our measurements. The latter line is density-dependent, and its larger size in Procyon is indicative of a lower density than the density of $\sim 10^{11} cm^{-3}$ in our electron beam ion trap. However, one of the strongest S VII lines, the 3d $\rightarrow$ 2p line at 60.2 Å (labelled VII-6 in Fig. 4 and Table 1, commonly referred to as 3C), is not seen in the *Chandra* data. Although this line is not on a chip gap, it is located between gaps in the -1 and +1 orders, and it might be affected by a reduced instrumental response function (R. Mewe private comm.). If, however, that line is indeed not present in the Procyon spectrum, which is unlikely, then S VII must be absent and the other lines near 72 Å would all be misidentified.

6. Conclusions

Our work here illustrates the need for careful laboratory measurements of isolated ions and elements in order to accurately identify and correlate emission lines with theoretical predictions. Most strong lines and some weaker lines can be identified with some confidence, as long as not too many different charge states are present. However, the density of weak lines prevents unequivocal identification of all lines, given the resolving power of our present instrumentation and the accuracy of the calculations. Despite these limitations, we find the laboratory spectra to be a useful aid for the analysis of spectra from *Chandra*. We are concerned with over-reliance on published databases that are compilations of theoretical calculations. As we have demonstrated, even the best atomic modelling codes must rely on laboratory measurements to get the correct numbers. We believe the measurements presented here are a significant step toward completely cataloguing astrophysically relevant EUV and soft X-ray ions. Future measurements using our new ultra high resolution grating spectrometer will enable us to make more precise measurements and should allow us to extend these measurements to ever weaker emission lines.

This work was supported by NASA Space Astrophysics Research and Analysis grant W-19,878 and was performed under the auspices of the Department of Energy by the University of California Lawrence Livermore National Laboratory under contract W-7405-ENG-48. E. B. was supported by grant No. 2002111 from the United States-Israel Binational Science Foundation (BSF), Jerusalem, Israel.

REFERENCES

Bar-Shalom, A., Klapisch, M., & Oreg, J. 2001, J. Quant. Spectrosc. & Rad. Transf., 71, 169.

Behar, E., Cottam, & Kahn, S. M. 2001, ApJ 548, 966

Beiersdorfer, P., Crespo Lpez-Urrutia, J. R., Springer, P., Utter, S. B., & Wong, K. L. 1999a, Rev. Sci. Instrum., 70, 276.

Beiersdorfer, P., Lepson, J. K., Brown, G. V., Utter, S. B., Kahn, S. M., Liedahl, D. A., & Mauche, C. W. 1999b, ApJ, 519, L185.

Beiersdorfer, P., Magee, E., Träbert, E., Chen, H., Lepson, J. K., Gu, M.-F., & Schmidt, M. 2004, Rev. Sci. Instrum. (in press).

Beiersdorfer, P., Scofield, J. H., & Osterheld, A. L. 2003, Phys. Rev. Lett. 90, 235003.

Brinkmann, A. C., Gunsing, C. J. T., Kaastra, J. S., van der Meer, R. L. J., Mewe, R., Paerels, F., Raasen, A. J. J., van Rooijen, J. J., Bräuninger, H., Burkert, W., Burwitz, V., Hartner, G., Predehl, P., Ness, J.-U., Schnmitt, J. H. M. M., Drake, J. J., Johnson, O., Juda, M., Kashyap, V., Murray, S. S., Pease, D., Ratzlaff, P., & Wargelin, B. J., 2000, ApJ 530, L111.

Brown, G. V., Beiersdorfer, P., Liedahl, D. A., Widmann, K., Kah, S. M., & Clothiaux, E. J. 2002, ApJ, 140, S589

Dere, K. P., Landi, E., Mason, H. E., Monsignori Fossi, B., & Young, P. R. 1997, A&AS, 125, 149.

Dere, K. P., Landi, E., Young, P. R., & Del Zanna, G. 2001, ApJ, 134, S331.

Doschek, G. A., & Cowan, R. D. 1984, ApJ, 56, S67.

Harada, T., & Kita, T. 1980, Appl. Opt., 19, 3987.

Kaastra, J. S., & Mewe, R. 1993, Legacy, 3, 6.

Kelly, R. L. 1987, Atomic and Ionic Spectrum Lines below 2000 Angstroms; Hydrogen through Krypton, J. Phys. Chem. Ref. Data, 16, Suppl. 1.

Klapisch, M., Schwob, J. L., Fraenkel, B. S., & Oreg, J. 1977, J. Opt. Soc. Am., 67, 148.

Lepson, J. K., Beiersdorfer, P., Brown, G. V., Chen, H., Gullikson, E. M., Schneider, M. B., Utter, S. B., & Wong , K. L. 2001, University of California Lawrence Livermore National Laboratory Report UCRL-ID-142264 [available at http://www.llnl.gov/tid/Library.html]

Lepson, J. K., Beiersdorfer, P., Brown, G. V., Liedahl, D. A., Utter, S. B., Brickhouse, N. S., Dupree, A. K., Kaastra, J. S., Mewe, R.,& Kahn, S. M. 2002, ApJ, 578, 648.

Lepson, J. K., Beiersdorfer, P., Behar, E.,& Kahn, S. M. 2003, ApJ, 590, 604.

Mewe, R., Kaastra, J. S., & Liedahl, D. A. 1995, Legacy, 6, 16.

Nakano, N., Kuroda, H., Kita, T., & Harada, T. 1984, Appl. Opt., 23, 2386.

Raassen, A. J. J., Mewe, R., Audard, M., Güdel, M., Kaastra, J. S., van der Meer, R. L. J., Foley, C. R., & Ness, J.-U., 2002, A&A, 389, 228.

Utter, S. B., Brown, G. V., Beiersdorfer, P., Clothiaux, E. G., & Podder, N. K., 1999, Rev. Sci. Instrum., 70, 284.

This preprint was prepared with the AAS LaTeX macros v5.0.

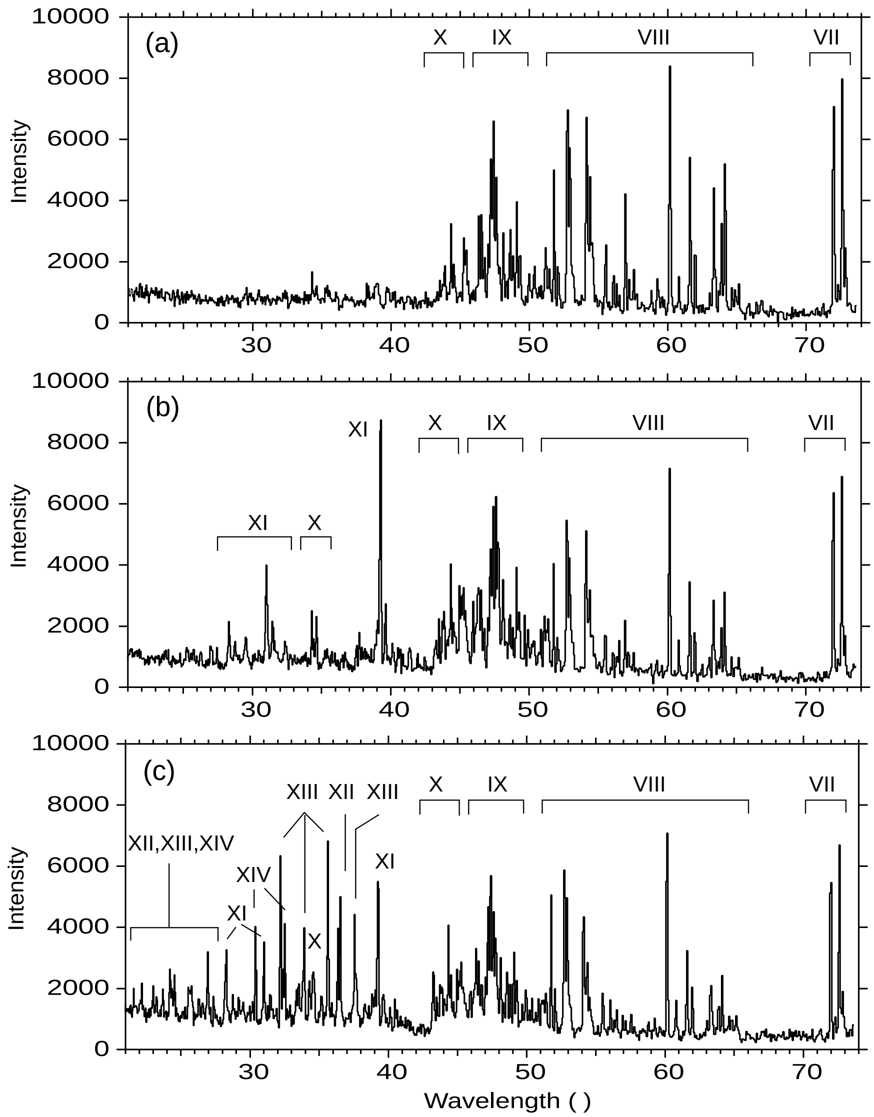

Fig. 1.— Spectra obtained with EBIT-II after subtraction of a constant stray light background. Note that each spectrum includes lines from several charge states. (a) Beam energy 300 eV. Dominant charge states are S VII, S VIII, and S IX. (b) Beam energy 450 eV. Charge states include S X and S XI. (c) Beam energy 730 eV. Charge states include S XII, S XIII, and S XIV

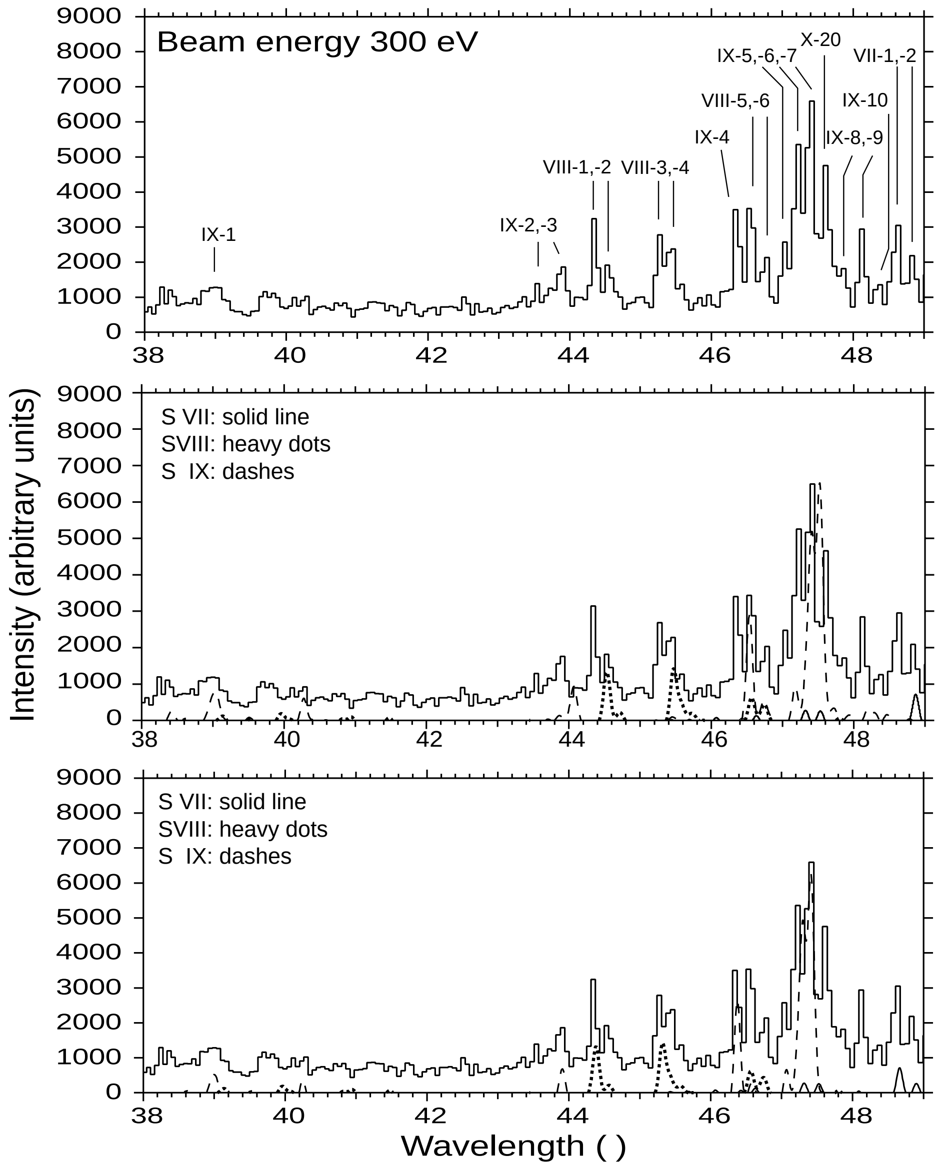

Fig. 2.— Comparison of EBIT-II spectrum and synthetic spectra constructed with HULLAC calculations. Beam energy is 300 eV, wavelength range 38–49 Å. Top: EBIT-II spectrum. Lack of lines near 42 Å is due to the carbon edge. Middle: EBIT-II data overlaid with synthetic HULLAC spectra, intensity adjusted for the detector response and normalized to the strongest measured peak in each charge state. Note that for some ions, the strongest peak is not in range of the graph. For example, the peak to which S VIII lines are normalized is found in Fig. 3. Bottom: EBIT-II overlaid with HULLAC, in which each line has been adjusted to match the experimentally determined position. This is the "best attempt" to reconcile theory with experiment.

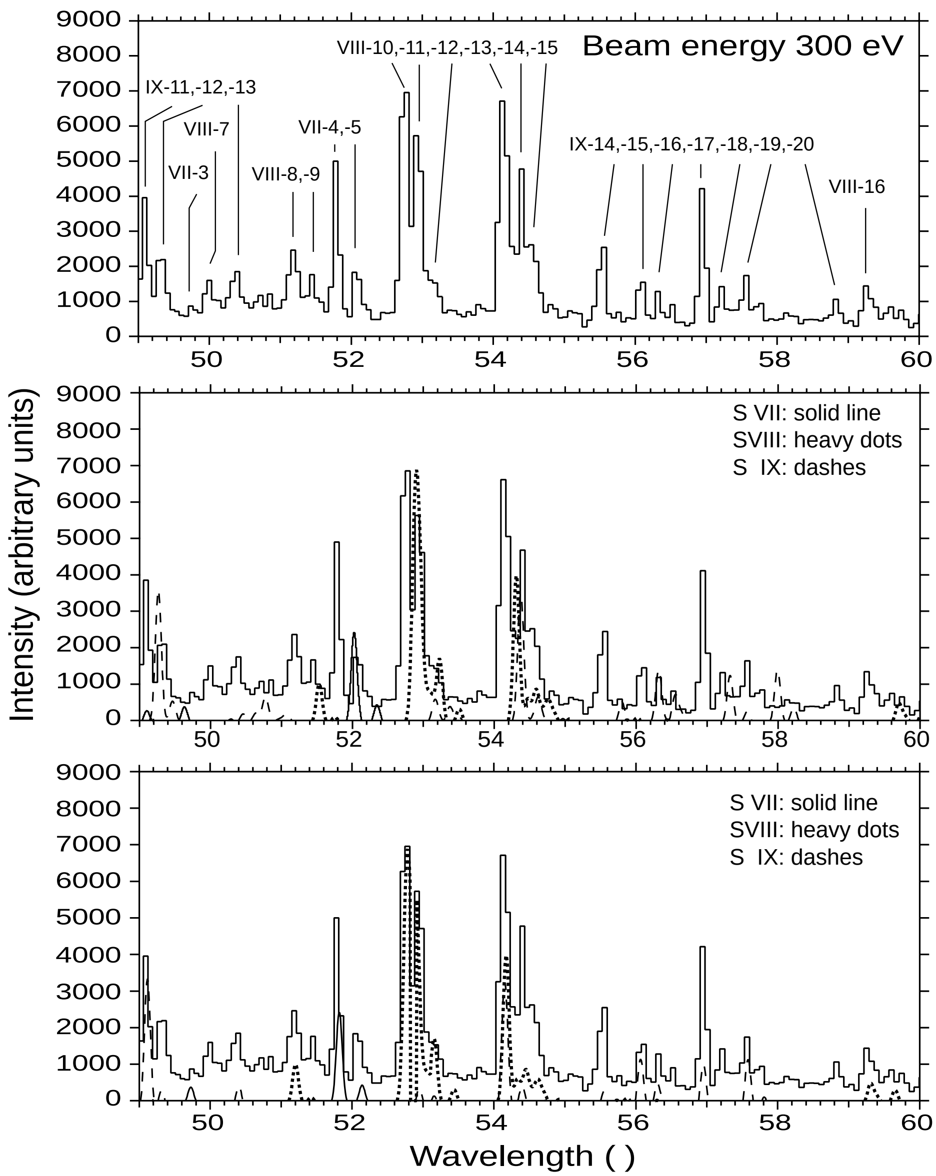

Fig. 3.— Comparison of EBIT-II spectrum and synthetic spectra constructed with HULLAC calculations. Beam energy is 300 eV, wavelength range 49–60 Å. Notations are the same as for Fig. 2.

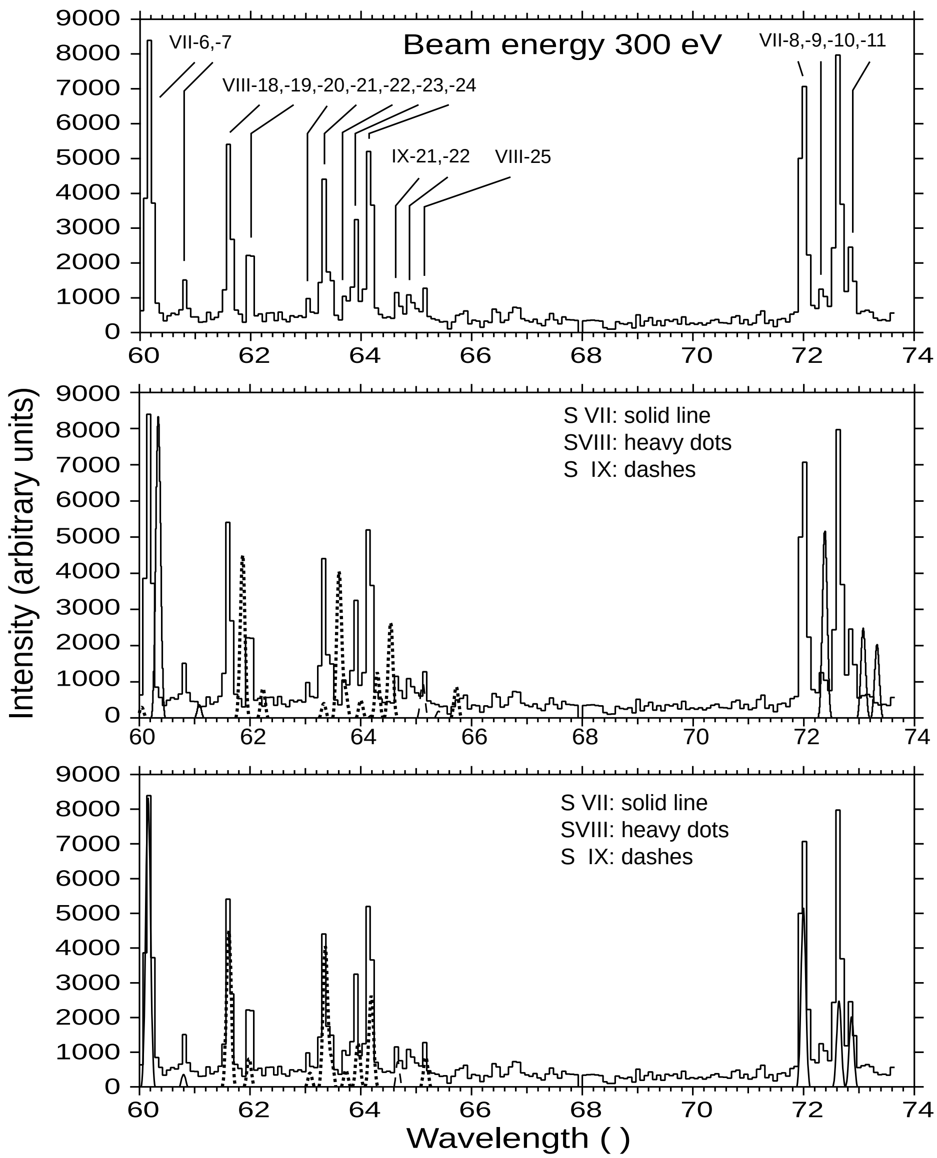

Fig. 4.— Comparison of EBIT-II spectrum and synthetic spectra constructed with HULLAC calculations. Beam energy is 300 eV, wavelength range 60–74 Å. Notations are the same as for Fig. 2.

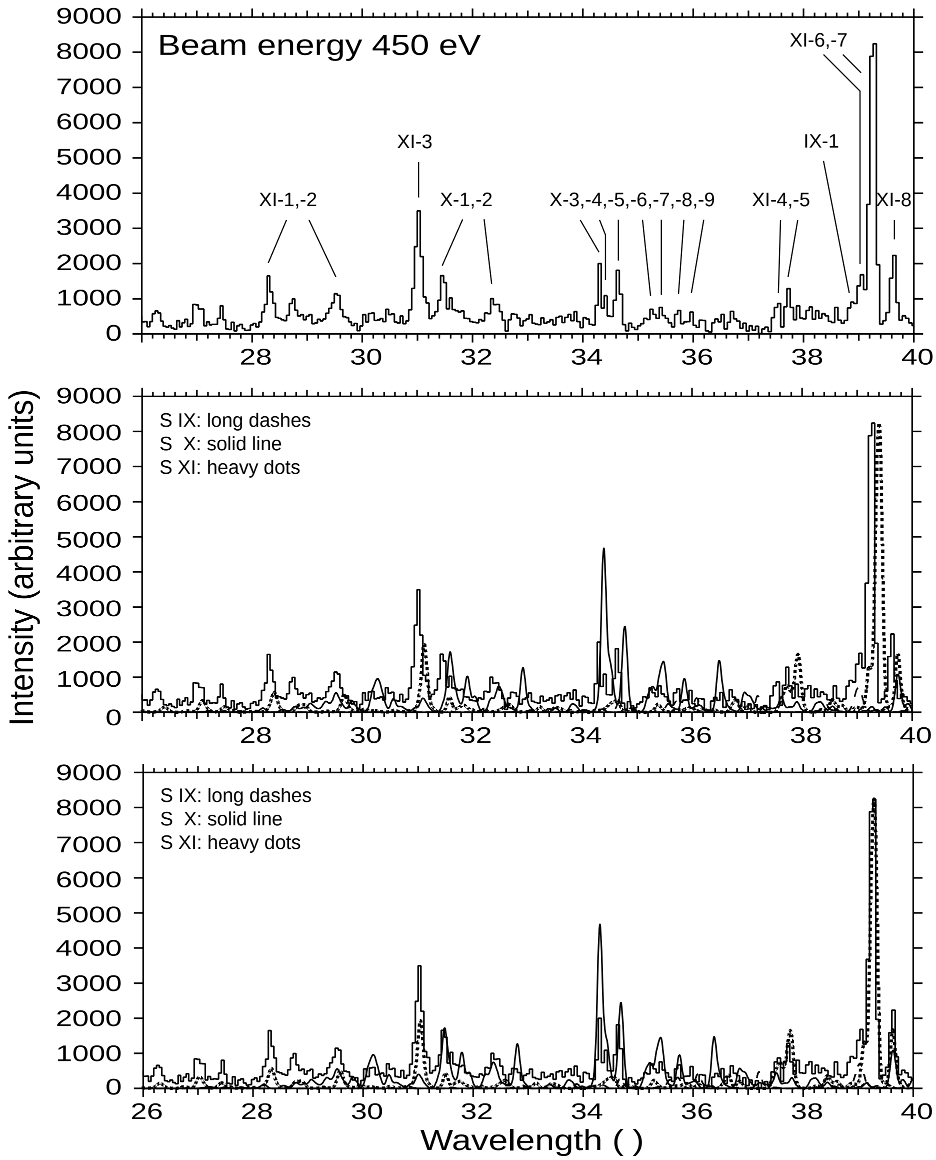

Fig. 5.— Comparison of EBIT-II spectrum and synthetic spectra constructed with HULLAC calculations. Beam energy is 450 eV, wavelength range 26–40 Å. Notations are the same as for Fig. 2.

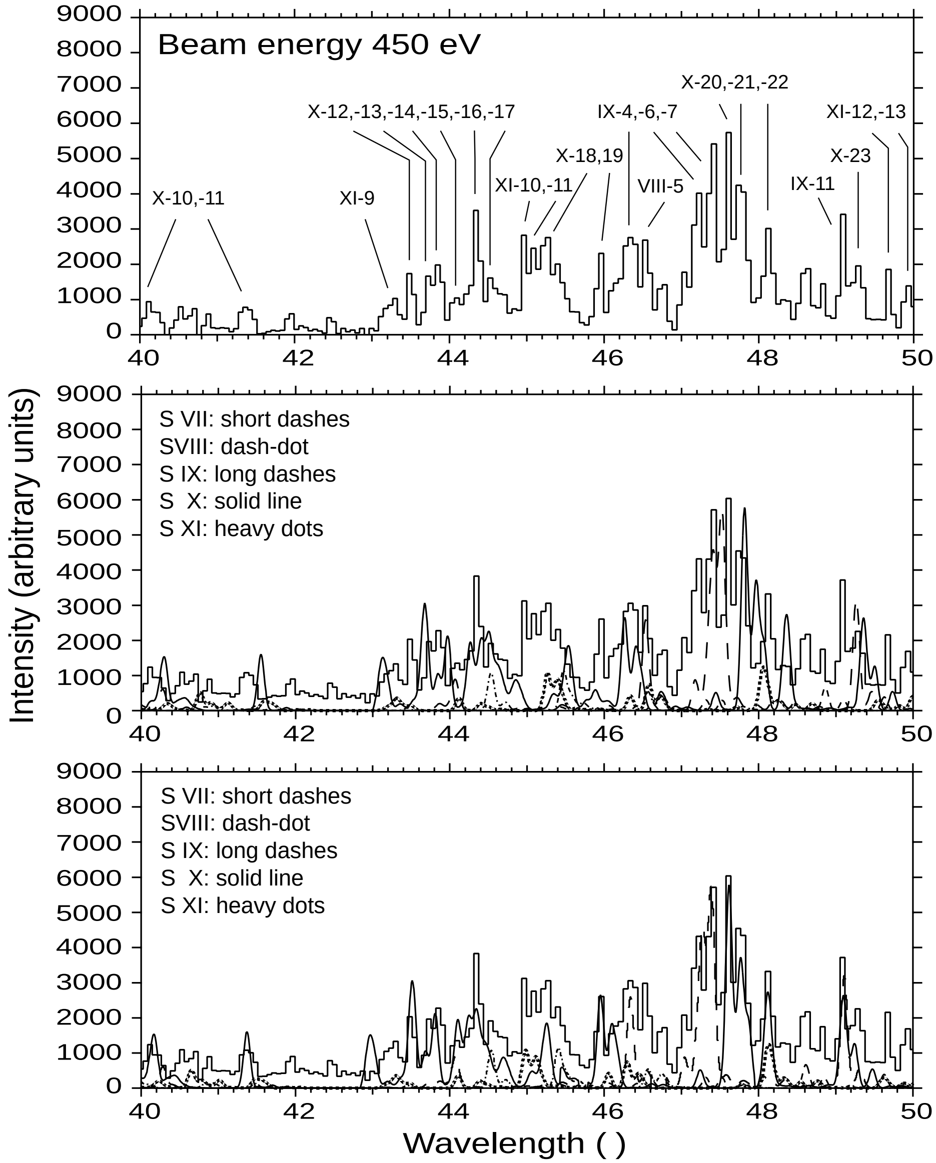

Fig. 6.— Comparison of EBIT-II spectrum and synthetic spectra constructed with HULLAC calculations. Beam energy is 450 eV, wavelength range 40–50 Å. Notations are the same as for Fig. 2.

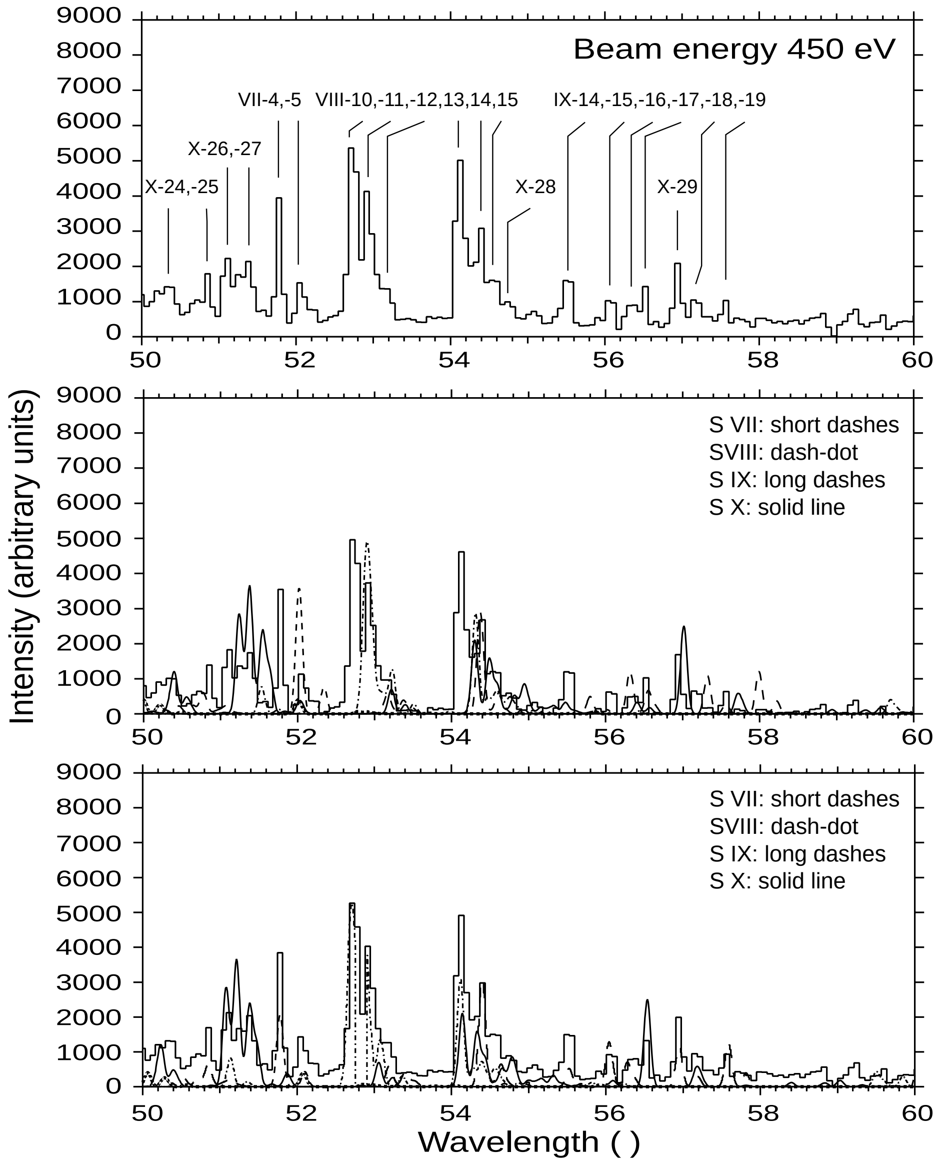

Fig. 7.— Comparison of EBIT-II spectrum and synthetic spectra constructed with HULLAC calculations. Beam energy is 450 eV, wavelength range 50–60 Å. Notations are the same as for Fig. 2.

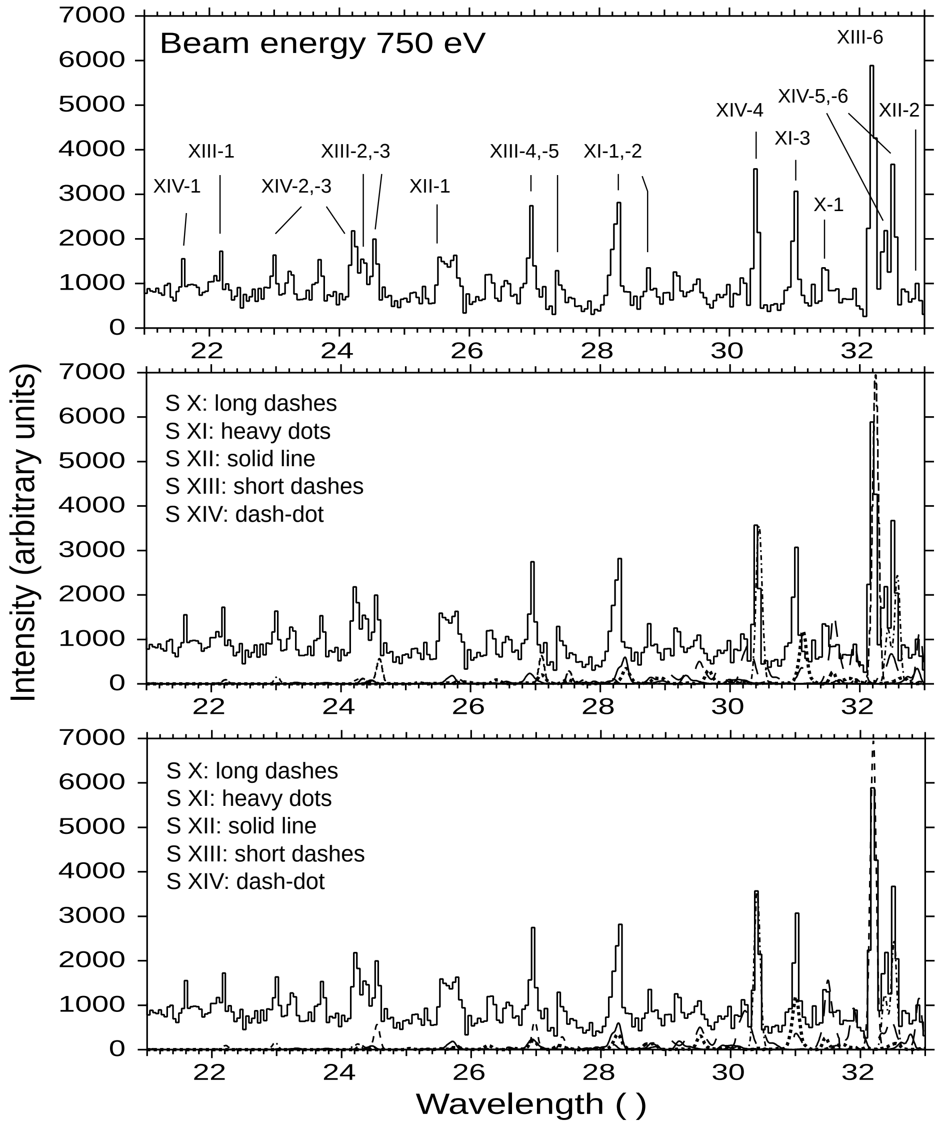

Fig. 8.— Comparison of EBIT-II spectrum and synthetic spectra constructed with HULLAC calculations. Beam energy is 750 eV, wavelength range 21-33 Å. Notations are the same as for Fig. 2.

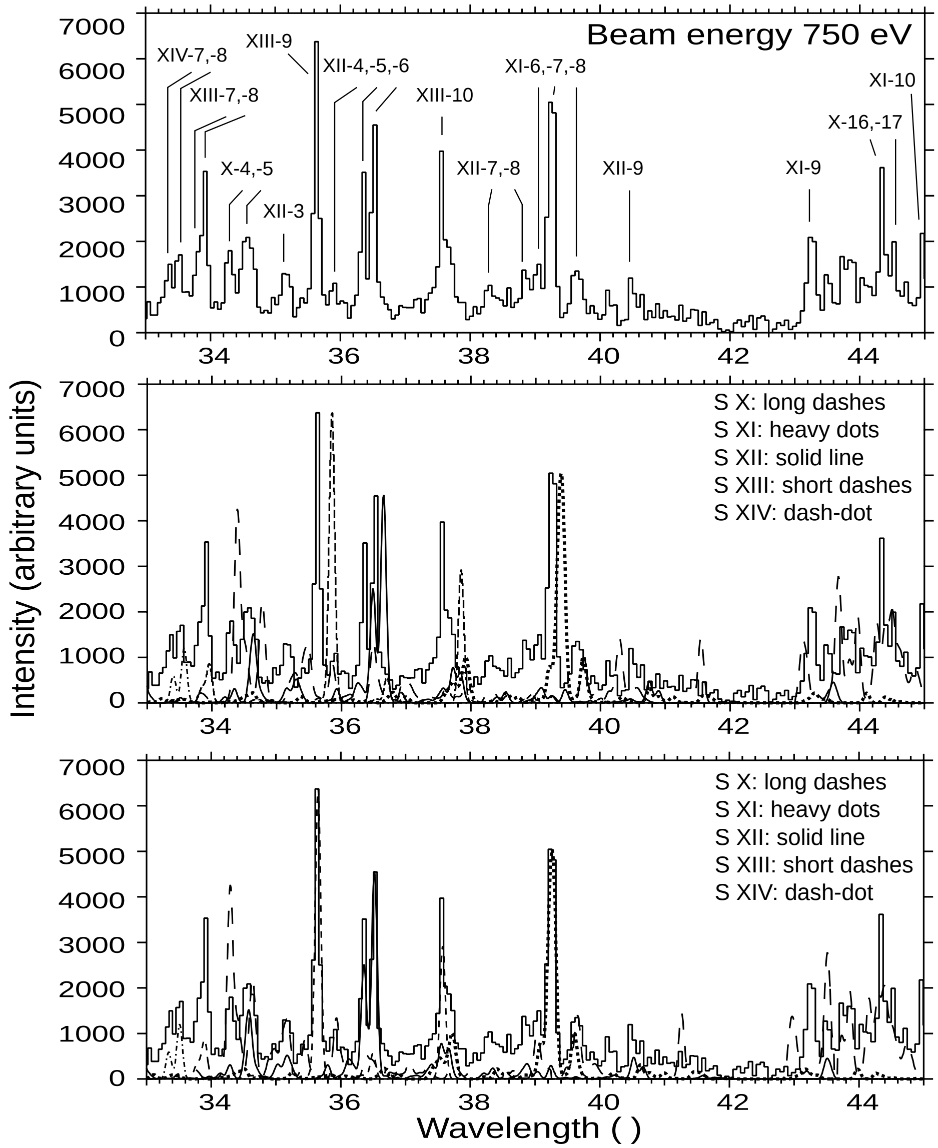

Fig. 9.— Comparison of EBIT-II spectrum and synthetic spectra constructed with HULLAC calculations. Beam energy is 750 eV, wavelength range 33-45 Å. Notations are the same as for Fig. 2.

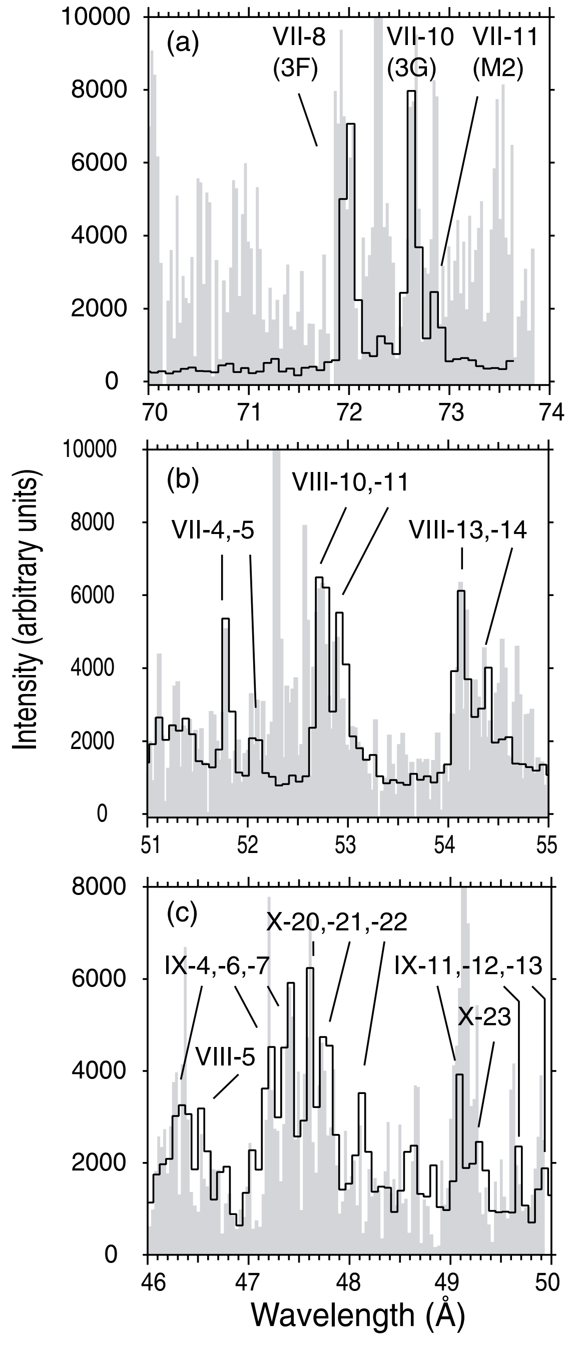

Fig. 10.— Comparison of EBIT-II sulfur spectra (black line) with *Chandra* spectrum of Procyon (gray fill). Strong EBIT-II lines are labelled as in the figures and tables. (a) Taken at beam energy of 300 eV, highlighting S VII. (b) Taken at beam energy of 400 eV, highlighting S VIII. (c) Taken at beam energy of 510 eV, highlighting S IX and S X.

Table 1. Summary of S VII emission data.

HULLAC Transition	HULLAC Intensity [a]	HULLAC λ (Å)	Feature	Measured Intensity [a]	Measured λ (Å)	St. Error	$\Delta\lambda$ [b]	MEKAL λ (Å) [c]	$\Delta\lambda$ [d]
$(1s^2 2s^2_{1/2} 2p_{1/2} 2p^4_{3/2} 5d_{3/2})_1 \rightarrow (1s^2 2s^2_{1/2} 2p^2_{1/2} 2p^4_{3/2})_0$	2	48.864	VII-1	3	48.639	0.003	0.225	...	...
...	1	49.099	VII-2	2	48.866	0.004	0.233	...	...
$(1s^2 2s_{1/2} 2p^2_{1/2} 2p^4_{3/2} 3p_{1/2})_1 \rightarrow (1s^2 2s^2_{1/2} 2p^2_{1/2} 2p^4_{3/2})_0$	1	49.628	VII-3	1	49.766	0.008	-0.138	50.000	0.234
$(1s^2 2s^2_{1/2} 2p_{1/2} 2p^4_{3/2} 4d_{3/2})_1 \rightarrow (1s^2 2s^2_{1/2} 2p^2_{1/2} 2p^4_{3/2})_0$	6	52.020	VII-4	8	51.820	0.002	0.200	51.807	-0.013
$(1s^2 2s^2_{1/2} 2p^2_{1/2} 2p^3_{3/2} 4d_{5/2})_1 \rightarrow (1s^2 2s^2_{1/2} 2p^2_{1/2} 2p^4_{3/2})_0$	1	52.342	VII-5	3	52.112	0.008	0.230	52.097	-0.015
$(1s^2 2s^2_{1/2} 2p_{1/2} 2p^4_{3/2} 3d_{3/2})_1 \rightarrow (1s^2 2s^2_{1/2} 2p^2_{1/2} 2p^4_{3/2})_0$	20	60.338	VII-6	19	60.203	0.003	0.135	60.610	0.407
$(1s^2 2s^2_{1/2} 2p^2_{1/2} 2p^3_{3/2} 3d_{5/2})_1 \rightarrow (1s^2 2s^2_{1/2} 2p^2_{1/2} 2p^4_{3/2})_0$	1	61.079	VII-7	3	60.851	0.003	0.228	60.807	-0.044
...	...	...	...	...	...	...	...	61.550	...
$(1s^2 2s^2_{1/2} 2p_{1/2} 2p^4_{3/2} 3s_{1/2})_1 \rightarrow (1s^2 2s^2_{1/2} 2p^2_{1/2} 2p^4_{3/2})_0$	13	72.376	VII-8	20	72.032	0.002	0.344	72.027	-0.005
$(1s^2 2s^2_{1/2} 2p_{1/2} 2p^4_{3/2} 3s_{1/2})_0 \rightarrow (1s^2 2s^2_{1/2} 2p^2_{1/2} 2p^4_{3/2})_0$	...	...	VII-9	3	72.375	0.006	...	...	...
$(1s^2 2s^2_{1/2} 2p^2_{1/2} 2p^3_{3/2} 3s_{1/2})_1 \rightarrow (1s^2 2s^2_{1/2} 2p^2_{1/2} 2p^4_{3/2})_0$	6	73.069	VII-10	18	72.662	0.002	0.407	72.663	0.001
$(1s^2 2s^2_{1/2} 2p^2_{1/2} 2p^3_{3/2} 3s_{1/2})_2 \rightarrow (1s^2 2s^2_{1/2} 2p^2_{1/2} 2p^4_{3/2})_0$	5	73.317	VII-11	6	72.891	0.002	0.426	...	...

[a] Relative to strongest peak, scale 1–20

[b] $\lambda_{HULLAC} - \lambda_{EBIT}$

[c] Kaastra & Mewe 1993; Mewe, Kaastra, & Liedahl 1995

[d] $\lambda_{MEKAL} - \lambda_{EBIT}$

Table 2. Summary of S VIII emission data.

HULLAC Transition	HULLAC Intensity [a]	HULLAC λ (Å)	Feature	Measured Intensity [a]	Measured λ (Å)	St. Error	$\Delta\lambda$ [b]	MEKAL λ (Å) [c]	$\Delta\lambda$ [d]	Comment
$(1s^22s^2_{1/2}2p_{1/2}2p^3_{3/2}5d_{3/2})_{3/2} \rightarrow (1s^22s^2_{1/2}2p^2_{1/2}2p^3_{3/2})_{3/2}$	1	42.392	...	...	...	...	...	...	...	carbon edge
$(1s^22s^2_{1/2}2p_{1/2}2p^3_{3/2}5d_{3/2})_{5/2} \rightarrow (1s^22s^2_{1/2}2p^2_{1/2}2p^3_{3/2})_{3/2}$	1	42.398	...	...	...	...	...	...	...	carbon edge
$(1s^22s^2_{1/2}2p^4_{3/2}5d_{5/2})_{5/2} \rightarrow (1s^22s^2_{1/2}2p^2_{1/2}2p^3_{3/2})_{3/2}$	2	42.332	...	...	...	...	...	...	...	carbon edge
$(1s^22s^2_{1/2}2p_{1/2}2p^3_{3/2}4d_{3/2})_{5/2} \rightarrow (1s^22s^2_{1/2}2p^2_{1/2}2p^3_{3/2})_{3/2}$	3	44.515	VIII-1	5 [e]	44.386	0.002	0.129	...	...	blend of 3 predicted lines
$(1s^22s^2_{1/2}2p_{1/2}2p^3_{3/2}4d_{5/2})_{3/2} \rightarrow (1s^22s^2_{1/2}2p^2_{1/2}2p^3_{3/2})_{3/2}$	2	44.541	VIII-1	5 [e]	44.386	0.002	0.155	...	...	blend of 3 predicted lines
$(1s^22s^2_{1/2}2p_{1/2}2p^3_{3/2}4d_{3/2})_{1/2} \rightarrow (1s^22s^2_{1/2}2p^2_{1/2}2p^3_{3/2})_{3/2}$	1	44.560	VIII-1	5 [e]	44.386	0.002	0.174	...	...	blend of 3 predicted lines
$(1s^22s^2_{1/2}2p_{1/2}2p^3_{3/2}4d_{3/2})_{3/2} \rightarrow (1s^22s^2_{1/2}2p_{1/2}2p^4_{3/2})_{1/2}$	< 1	44.685	VIII-2	3 [e]	44.566	0.005	0.119	...	...	blend of 2 predicted lines
$(1s^22s^2_{1/2}2p_{1/2}2p^3_{3/2}4d_{5/2})_{3/2} \rightarrow (1s^22s^2_{1/2}2p_{1/2}2p^4_{3/2})_{1/2}$	1	44.734	VIII-2	3 [e]	44.566	0.005	0.168	...	...	blend of 2 predicted lines
$(1s^22s^2_{1/2}2p^4_{3/2}4d_{5/2})_{5/2} \rightarrow (1s^22s^2_{1/2}2p^2_{1/2}2p^3_{3/2})_{3/2}$	6	45.468	VIII-3	3	45.287	0.004	0.181	45.300	0.013	...
$(1s^22s^2_{1/2}2p_{1/2}2p^3_{3/2}4d_{3/2})_{3/2} \rightarrow (1s^22s^2_{1/2}2p^2_{1/2}2p^3_{3/2})_{3/2}$	2	45.557	VIII-4	7	45.457	0.005	0.100	46.000	0.543	...
$(1s^22s^2_{1/2}2p_{1/2}2p^3_{3/2}4s_{1/2})_{5/2} \rightarrow (1s^22s^2_{1/2}2p^2_{1/2}2p^3_{3/2})_{3/2}$	2	46.565	VIII-5	4	46.726	0.003	-0.161	...	...	blend w/ IX
$(1s^22s_{1/2}2p^2_{1/2}2p^3_{3/2}3p_{3/2})_{5/2} \rightarrow (1s^22s^2_{1/2}2p^2_{1/2}2p^3_{3/2})_{3/2}$	2	46.752	VIII-6	4	46.789	0.002	-0.037	...	...	...
...	...	...	VIII-7	2	50.005	0.008	...	...	...	...
$(1s^22s^2_{1/2}2p^2_{1/2}2p^2_{3/2}3d_{5/2})_{5/2} \rightarrow (1s^22s^2_{1/2}2p^2_{1/2}2p^3_{3/2})_{3/2}$	4	51.533	VIII-8	3	51.272	0.008	0.261	...	...	...
$(1s^22s^2_{1/2}2p^2_{1/2}2p^2_{3/2}3d_{3/2})_{3/2} \rightarrow (1s^22s^2_{1/2}2p_{1/2}2p^4_{3/2})_{1/2}$	< 1	51.762	VIII-9	2	51.469	0.007	0.293	...	...	...
$(1s^22s^2_{1/2}2p_{1/2}2p^3_{3/2}3d_{3/2})_{5/2} \rightarrow (1s^22s^2_{1/2}2p^2_{1/2}2p^3_{3/2})_{3/2}$	20	52.884	VIII-10	20	52.781	0.002	0.103	52.854	0.073	...
$(1s^22s^2_{1/2}2p_{1/2}2p^3_{3/2}3d_{5/2})_{3/2} \rightarrow (1s^22s^2_{1/2}2p^2_{1/2}2p^3_{3/2})_{3/2}$	14	52.947	VIII-11	14	52.973	0.002	-0.026	...	...	...
$(1s^22s^2_{1/2}2p_{1/2}2p^3_{3/2}3d_{3/2})_{3/2} \rightarrow (1s^22s^2_{1/2}2p_{1/2}2p^4_{3/2})_{1/2}$	2	53.066	VIII-12	2 [e]	53.222	0.009	-0.156	...	...	blend of 4 predicted lines; shoulder
$(1s^22s^2_{1/2}2p_{1/2}2p^3_{3/2}3d_{5/2})_{1/2} \rightarrow (1s^22s^2_{1/2}2p_{1/2}2p^4_{3/2})_{1/2}$	2	53.125	VIII-12	2 [e]	53.222	0.009	-0.097	...	...	blend of 4 predicted lines; shoulder
$(1s^22s^2_{1/2}2p_{1/2}2p^3_{3/2}3d_{5/2})_{3/2} \rightarrow (1s^22s^2_{1/2}2p_{1/2}2p^4_{3/2})_{1/2}$	2	53.219	VIII-12	2 [e]	53.222	0.009	-0.003	...	...	blend of 4 predicted lines; shoulder
$(1s^22s^2_{1/2}2p_{1/2}2p^3_{3/2}3d_{3/2})_{3/2} \rightarrow (1s^22s^2_{1/2}2p^2_{1/2}2p^3_{3/2})_{3/2}$	5	53.233	VIII-12	2 [e]	53.222	0.009	0.011	...	...	blend of 4 predicted lines; shoulder
$(1s^22s^2_{1/2}2p^4_{3/2}3d_{5/2})_{5/2} \rightarrow (1s^22s^2_{1/2}2p^2_{1/2}2p^3_{3/2})_{3/2}$	16	54.312	VIII-13	11	54.162	0.003	0.150	54.118	-0.044	blend w/ X
$(1s^22s^2_{1/2}2p^2_{1/2}2p^2_{3/2}3d_{5/2})_{3/2} \rightarrow (1s^22s^2_{1/2}2p^2_{1/2}2p^3_{3/2})_{3/2}$	3	54.471	VIII-14	8 [e]	54.415	0.003	0.056	...	...	blend of 2 predicted lines
$(1s^22s^2_{1/2}2p_{1/2}2p^3_{3/2}3d_{5/2})_{5/2} \rightarrow (1s^22s^2_{1/2}2p^2_{1/2}2p^3_{3/2})_{3/2}$	3	54.589	VIII-14	8 [e]	54.415	0.003	0.174	...	...	blend of 2 predicted lines
$(1s^22s^2_{1/2}2p^2_{1/2}2p^2_{3/2}3d_{5/2})_{3/2} \rightarrow (1s^22s^2_{1/2}2p_{1/2}2p^4_{3/2})_{1/2}$	2	54.759	VIII-15	6	54.601	0.003	0.158	...	...	...
$(1s^22s^2_{1/2}2p^2_{1/2}2p^2_{3/2}3s_{1/2})_{1/2} \rightarrow (1s^22s^2_{1/2}2p^2_{1/2}2p^3_{3/2})_{3/2}$	2	59.698	VIII-16	3	59.308	0.004	0.390	...	...	...
$(1s^22s^2_{1/2}2p^2_{1/2}2p^2_{3/2}3s_{1/2})_{1/2} \rightarrow (1s^22s^2_{1/2}2p_{1/2}2p^4_{3/2})_{1/2}$	2	60.044	VIII-17	2	59.624	0.013	0.420	...	...	...
$(1s^22s^2_{1/2}2p_{1/2}2p^3_{3/2}3s_{1/2})_{5/2} \rightarrow (1s^22s^2_{1/2}2p^2_{1/2}2p^3_{3/2})_{3/2}$	17	61.866	VIII-18	15	61.645	0.002	0.221	61.600	-0.045	...
$(1s^22s^2_{1/2}2p_{1/2}2p^3_{3/2}3s_{1/2})_{3/2} \rightarrow (1s^22s^2_{1/2}2p_{1/2}2p^4_{3/2})_{1/2}$	4	62.232	VIII-19	6	62.029	0.001	0.203	...	...	...
$(1s^22s^2_{1/2}2p_{1/2}2p^3_{3/2}3s_{1/2})_{1/2} \rightarrow (1s^22s^2_{1/2}2p^2_{1/2}2p^3_{3/2})_{3/2}$	2	63.332	VIII-20	2	63.061	0.004	0.271	...	...	...
$(1s^22s^2_{1/2}2p^2_{1/2}2p^2_{3/2}3s_{1/2})_{3/2} \rightarrow (1s^22s^2_{1/2}2p^2_{1/2}2p^3_{3/2})_{3/2}$	16	63.608	VIII-21	10 [e]	63.365	0.002	0.243	63.204	-0.061	blend of 2 predicted lines
$(1s^22s^2_{1/2}2p_{1/2}2p^3_{3/2}3s_{1/2})_{1/2} \rightarrow (1s^22s^2_{1/2}2p_{1/2}2p^4_{3/2})_{1/2}$	3	63.722	VIII-21	10 [e]	63.365	0.002	0.357	63.304	-0.061	blend of 2 predicted lines
$(1s^22s^2_{1/2}2p^2_{1/2}2p^2_{3/2}3s_{1/2})_{3/2} \rightarrow (1s^22s^2_{1/2}2p_{1/2}2p^4_{3/2})_{1/2}$	2	64.001	VIII-22	2	63.784	0.010	0.217	...	...	...
$(1s^22s^2_{1/2}2p_{1/2}2p^3_{3/2}3s_{1/2})_{3/2} \rightarrow (1s^22s^2_{1/2}2p^2_{1/2}2p^3_{3/2})_{3/2}$	5	64.299	VIII-23	7	63.935	0.003	0.364	...	...	...
$(1s^22s^2_{1/2}2p^2_{1/2}2p^2_{3/2}3s_{1/2})_{5/2} \rightarrow (1s^22s^2_{1/2}2p^2_{1/2}2p^3_{3/2})_{3/2}$	8	64.536	VIII-24	16 [e]	64.185	0.002	0.351	...	...	blend of 2 predicted lines
$(1s^22s^2_{1/2}2p^4_{3/2}3s_{1/2})_{1/2} \rightarrow (1s^22s^2_{1/2}2p_{1/2}2p^4_{3/2})_{1/2}$	2	64.553	VIII-24	16 [e]	64.185	0.002	0.368	...	...	blend of 2 predicted lines
$(1s^22s_{1/2}2p^2_{1/2}2p^3_{3/2}3s_{1/2})_{3/2} \rightarrow (1s^22s_{1/2}2p^2_{1/2}2p^4_{3/2})_{1/2}$	4	65.725	VIII-25	3	65.194	0.005	0.531	...	...	...

[a] Relative to strongest peak, scale 1–20

[b] $\lambda_{HULLAC} - \lambda_{EBIT}$

[c] Kaastra & Mewe 1993; Mewe, Kaastra, & Liedahl 1995

[d] $\lambda_{MEKAL} - \lambda_{EBIT}$

[e] Combined intensity of blended feature

Table 3. Summary of S IX emission data.

HULLAC Transition	HULLAC Intensity [a]	HULLAC λ (Å)	Feature	Measured Intensity [a]	Measured λ (Å)	St. Error	$\Delta\lambda$ [b]	MEKAL λ (Å) [c]	$\Delta\lambda$ [d]	Comment
$(1s^2 2s^2_{1/2} 2p^3_{3/2} 5d_{5/2})_6 \rightarrow (1s^2 2s^2_{1/2} 2p^2_{1/2} 2p^2_{3/2})_4$	1	35.559	...	...	...	...	...	...	...	...
$(1s^2 2s^2_{1/2} 2p^3_{3/2} 6d_{3/2})_6 \rightarrow (1s^2 2s^2_{1/2} 2p^2_{1/2} 2p^2_{3/2})_4$	1	35.722	...	...	...	...	...	...	...	...
$(1s^2 2s^2_{1/2} 2p_{1/2} 2p^2_{3/2} 5d_{3/2})_4 \rightarrow (1s^2 2s^2_{1/2} 2p^2_{1/2} 2p^2_{3/2})_4$	1	36.071	...	...	...	...	...	...	...	...
$(1s^2 2s^2_{1/2} 2p_{1/2} 2p^2_{3/2} 5d_{5/2})_6 \rightarrow (1s^2 2s^2_{1/2} 2p^2_{1/2} 2p^2_{3/2})_4$	1	36.106	...	...	...	...	...	...	...	...
$(1s^2 2s^2_{1/2} 2p_{1/2} 2p^2_{3/2} 5d_{5/2})_6 \rightarrow (1s^2 2s^2_{1/2} 2p^2_{1/2} 2p^2_{3/2})_4$	2	37.192	...	...	...	...	...	...	...	...
$(1s^2 2s^2_{1/2} 2p^3_{3/2} 4d_{5/2})_6 \rightarrow (1s^2 2s^2_{1/2} 2p^2_{1/2} 2p^2_{3/2})_4$	2	38.419	...	...	...	...	...	...	...	...
$(1s^2 2s^2_{1/2} 2p^3_{3/2} 4d_{3/2})_2 \rightarrow (1s^2 2s^2_{1/2} 2p^2_{1/2} 2p^2_{3/2})_4$	1	38.929	IX-1	1 [e]	39.085	0.007	-0.156	39.460	0.375	blend of 3 predicted lines
$(1s^2 2s^2_{1/2} 2p_{1/2} 2p^2_{3/2} 4d_{5/2})_4 \rightarrow (1s^2 2s^2_{1/2} 2p^2_{1/2} 2p^2_{3/2})_4$	3	38.996	IX-1	1 [e]	39.085	0.007	-0.089	39.460	0.375	blend of 3 predicted lines
$(1s^2 2s^2_{1/2} 2p_{1/2} 2p^2_{3/2} 4d_{5/2})_6 \rightarrow (1s^2 2s^2_{1/2} 2p^2_{1/2} 2p^2_{3/2})_4$	3	39.06	IX-1	1 [e]	39.085	0.007	-0.025	39.460	0.375	blend of 3 predicted lines
$(1s^2 2s_{1/2} 2p^2_{1/2} 2p^2_{3/2} 3p_{3/2})_6 \rightarrow (1s^2 2s^2_{1/2} 2p^2_{1/2} 2p^2_{3/2})_4$	1	39.508	...	...	...	...	...	...	...	...
$(1s^2 2s_{1/2} 2p_{1/2} 2p^3_{3/2} 4p_{3/2})_6 \rightarrow (1s^2 2s^2_{1/2} 2p^2_{1/2} 2p^2_{3/2})_4$	4	40.277	...	...	...	...	...	...	...	blend w/ X
$(1s^2 2s^2_{1/2} 2p^2_{1/2} 2p_{3/2} 4d_{5/2})_4 \rightarrow (1s^2 2s^2_{1/2} 2p_{1/2} 2p^3_{3/2})_2$	1	40.404	...	...	...	...	...	...	...	...
$(1s^2 2s^2_{1/2} 2p_{1/2} 2p^2_{3/2} 4s_{1/2})_6 \rightarrow (1s^2 2s^2_{1/2} 2p^2_{1/2} 2p^2_{3/2})_4$	1	40.584	...	...	...	...	...	...	...	...
$(1s^2 2s_{1/2} 2p_{1/2} 2p^3_{3/2} 3p_{1/2})_4 \rightarrow (1s^2 2s^2_{1/2} 2p^2_{1/2} 2p^2_{3/2})_4$	1	43.706	...	...	...	...	...	...	...	...
$(1s^2 2s_{1/2} 2p_{1/2} 2p^3_{3/2} 3p_{1/2})_4 \rightarrow (1s^2 2s^2_{1/2} 2p_{1/2} 2p^3_{3/2})_2$	1	43.847	IX-2	1 [e]	43.765	0.011	0.082	...	...	blend of 2 predicted lines, with X
$(1s^2 2s_{1/2} 2p^2_{1/2} 2p^2_{3/2} 3p_{1/2})_2 \rightarrow (1s^2 2s^2_{1/2} 2p^2_{1/2} 2p^2_{3/2})_4$	1	43.877	IX-2	1 [e]	43.765	0.011	0.112	...	...	blend of 2 predicted lines, with X
$(1s^2 2s_{1/2} 2p^2_{1/2} 2p^2_{3/2} 3p_{1/2})_6 \rightarrow (1s^2 2s^2_{1/2} 2p^2_{1/2} 2p^2_{3/2})_4$	4	44.066	IX-3	1	43.891	0.007	0.175	...	...	blend w/ X
$(1s^2 2s_{1/2} 2p_{1/2} 2p^3_{3/2} 3p_{1/2})_4 \rightarrow (1s^2 2s^2_{1/2} 2p_{1/2} 2p^3_{3/2})_2$	1	44.115	...	...	...	...	...	...	...	...
$(1s^2 2s_{1/2} 2p_{1/2} 2p^3_{3/2} 3d_{5/2})_6 \rightarrow (1s^2 2s_{1/2} 2p^2_{1/2} 2p^3_{3/2})_4$	1	45.453	...	...	...	...	...	...	...	...
$(1s^2 2s^2_{1/2} 2p^3_{3/2} 3d_{5/2})_6 \rightarrow (1s^2 2s^2_{1/2} 2p^2_{1/2} 2p^2_{3/2})_4$	10	46.535	IX-4	7	46.383	0.004	0.152	...	...	...
$(1s^2 2s^2_{1/2} 2p_{1/2} 2p^2_{3/2} 3d_{5/2})_4 \rightarrow (1s^2 2s^2_{1/2} 2p_{1/2} 2p^3_{3/2})_2$	2	46.726	...	3	46.592	0.003	0.134	...	...	blend w/ VIII-6
$(1s^2 2s^2_{1/2} 2p_{1/2} 2p^2_{3/2} 3d_{5/2})_6 \rightarrow (1s^2 2s^2_{1/2} 2p^2_{1/2} 2p^2_{3/2})_4$	1	46.801	...	...	...	...	...	...	...	...
$(1s^2 2s^2_{1/2} 2p^2_{1/2} 2p_{3/2} 3d_{5/2})_2 \rightarrow (1s^2 2s^2_{1/2} 2p^2_{1/2} 2p^2_{3/2})_4$	4	47.178	...	...	...	...	...	...	...	...
$(1s^2 2s^2_{1/2} 2p_{1/2} 2p^2_{3/2} 3d_{3/2})_2 \rightarrow (1s^2 2s^2_{1/2} 2p^2_{1/2} 2p^2_{3/2})_4$	3	47.333	IX-5	3	47.078	0.005	0.255	...	...	...
$(1s^2 2s^2_{1/2} 2p^2_{1/2} 2p_{3/2} 3d_{5/2})_2 \rightarrow (1s^2 2s^2_{1/2} 2p_{1/2} 2p^3_{3/2})_2$	2	47.342	...	...	...	...	...	...	...	...
$(1s^2 2s^2_{1/2} 2p^2_{1/2} 2p_{3/2} 3d_{5/2})_2 \rightarrow (1s^2 2s^2_{1/2} 2p^4_{3/2})_0$	1	47.406	...	...	...	...	...	...	...	...
$(1s^2 2s^2_{1/2} 2p^3_{3/2} 3d_{5/2})_4 \rightarrow (1s^2 2s^2_{1/2} 2p^2_{1/2} 2p^2_{3/2})_4$	16	47.41	IX-6	16	47.256	0.004	0.154	...	...	...
$(1s^2 2s^2_{1/2} 2p_{1/2} 2p^2_{3/2} 3d_{3/2})_2 \rightarrow (1s^2 2s^2_{1/2} 2p_{1/2} 2p^3_{3/2})_2$	1	47.498	...	...	...	...	...	...	...	...
$(1s^2 2s^2_{1/2} 2p_{1/2} 2p^2_{3/2} 3d_{5/2})_6 \rightarrow (1s^2 2s^2_{1/2} 2p^2_{1/2} 2p^2_{3/2})_4$	20	47.521	IX-7	20	47.436	0.001	0.085	47.500	0.064	...
$(1s^2 2s^2_{1/2} 2p_{1/2} 2p^2_{3/2} 3d_{3/2})_2 \rightarrow (1s^2 2s^2_{1/2} 2p^4_{3/2})_0$	1	47.562	...	...	...	...	...	...	...	...
$(1s^2 2s^2_{1/2} 2p^3_{3/2} 3d_{53/2})_4 \rightarrow (1s^2 2s^2_{1/2} 2p_{1/2} 2p^3_{3/2})_2$	2	47.576	...	...	...	...	...	...	...	...
$(1s^2 2s^2_{1/2} 2p_{1/2} 2p^2_{3/2} 3d_{5/2})_4 \rightarrow (1s^2 2s^2_{1/2} 2p_{1/2} 2p^3_{3/2})_2$	1	47.711	...	...	...	...	...	...	...	...
$(1s^2 2s^2_{1/2} 2p_{1/2} 2p^2_{3/2} 3d_{5/2})_6 \rightarrow (1s^2 2s^2_{1/2} 2p_{1/2} 2p^3_{3/2})_4$	1	48.193	IX-8	3	47.818	0.013	0.375	...	...	...
$(1s^2 2s^2_{1/2} 2p^2_{1/2} 2p_{3/2} 3d_{5/2})_6 \rightarrow (1s^2 2s^2_{1/2} 2p_{1/2} 2p^3_{3/2})_4$	1	48.299	IX-9	7	48.158	0.002	0.141	...	...	...
$(1s^2 2s^2_{1/2} 2p_{1/2} 2p^2_{3/2} 4p_{3/2})_4 \rightarrow (1s^2 2s_{1/2} 2p^2_{1/2} 2p^3_{3/2})_4$	1	48.465	IX-10	2	48.377	0.006	0.088	...	...	...
$(1s^2 2s^2_{1/2} 2p_{1/2} 2p^2_{3/2} 3d_{5/2})_6 \rightarrow (1s^2 2s^2_{1/2} 2p^2_{1/2} 2p^2_{3/2})_4$	13	49.265	IX-11	9 [e]	49.127	0.003	0.138	...	...	blend of 2 predicted lines
$(1s^2 2s^2_{1/2} 2p^2_{1/2} 2p_{3/2} 3d_{5/2})_4 \rightarrow (1s^2 2s^2_{1/2} 2p^2_{1/2} 2p^2_{3/2})_4$	1	49.284	IX-11	9 [e]	49.127	0.003	0.157	...	...	blend of 2 predicted lines
$(1s^2 2s^2_{1/2} 2p^2_{1/2} 2p_{3/2} 3d_{5/2})_4 \rightarrow (1s^2 2s^2_{1/2} 2p_{1/2} 2p^3_{3/2})_2$	2	49.463	IX-12	6	49.326	0.004	0.137	...	...	...
$(1s^2 2s^2_{1/2} 2p^2_{1/2} 2p_{3/2} 4p_{3/2})_4 \rightarrow (1s^2 2s_{1/2} 2p_{1/2} 2p^4_{3/2})_2$	1	50.46	...	...	...	...	...	...	...	...
$(1s^2 2s_{1/2} 2p^2_{1/2} 2p^2_{3/2} 3d_{5/2})_6 \rightarrow (1s^2 2s_{1/2} 2p^2_{1/2} 2p^3_{3/2})_4$	1	50.641	...	...	...	...	...	...	...	...
$(1s^2 2p_{1/2} 2p^4_{3/2} 3p_{3/2})_4 \rightarrow (1s^2 2s_{1/2} 2p^2_{1/2} 2p^3_{3/2})_4$	2	50.766	IX-13	7	50.398	0.006	0.368	...	...	...
$(1s^2 2s_{1/2} 2p_{1/2} 2p^3_{3/2} 3d_{5/2})_4 \rightarrow (1s^2 2s_{1/2} 2p_{1/2} 2p^4_{3/2})_2$	1	50.781	...	...		...	...	...	...	...
$(1s^2 2s_{1/2} 2p_{1/2} 2p^3_{3/2} 3d_{5/2})_6 \rightarrow (1s^2 2s_{1/2} 2p^2_{1/2} 2p^3_{3/2})_4$	1	51.063	...	...		...	...	...	...	...
$(1s^2 2s^2_{1/2} 2p^3_{3/2} 3s_{1/2})_4 \rightarrow (1s^2 2s^2_{1/2} 2p^2_{1/2} 2p^2_{3/2})_4$	2	53.162	...	...	52.973	0.002	0.189	...	...	blend w/ VIII-10
$(1s^2 2s^2_{1/2} 2p^3_{3/2} 3s_{1/2})_4 \rightarrow (1s^2 2s^2_{1/2} 2p_{1/2} 2p^3_{3/2})_2$	2	53.37	...	...	...	...	...	...	...	blend of 2 predicted lines, w/ VIII-11
$(1s^2 2s^2_{1/2} 2p_{1/2} 2p^2_{3/2} 3s_{1/2})_2 \rightarrow (1s^2 2s^2_{1/2} 2p^4_{3/2})_0$	1	53.504	...	...	...	...	...	...	...	blend of 2 predicted lines, w/ VIII-11
$(1s^2 2s^2_{1/2} 2p_{1/2} 2p^2_{3/2} 3s_{1/2})_6 \rightarrow (1s^2 2s^2_{1/2} 2p^2_{1/2} 2p^2_{3/2})_4$	12	54.37	...	...	54.162	0.003	0.208	54.180	0.018	blend w/ VIII-13

Table 3—Continued

HULLAC Transition	HULLAC Intensity [a]	HULLAC λ (Å)	Feature	Measured Intensity [a]	Measured λ (Å)	St. Error	$\Delta\lambda$ [b]	MEKAL λ (Å) [c]	$\Delta\lambda$ [d]	Comment
$(1s^2 2s^2_{1/2} 2p_{1/2} 2p^2_{3/2} 3s_{1/2})_2 \rightarrow (1s^2 2s^2_{1/2} 2p^2_{1/2} 2p^2_{3/2})_4$	5	56.316	IX-15	3	56.108	0.002	0.208	...	...	...
$(1s^2 2s^2_{1/2} 2p_{1/2} 2p^2_{3/2} 3s_{1/2})_4 \rightarrow (1s^2 2s^2_{1/2} 2p_{1/2} 2p^3_{3/2})_2$	3	56.55	IX-16	2	56.369	0.012	0.181	...	...	...
$(1s^2 2s^2_{1/2} 2p_{1/2} 2p^2_{3/2} 3s_{1/2})_2 \rightarrow (1s^2 2s^2_{1/2} 2p^4_{3/2})_0$	1	56.641	...	...	...	...	...	...	...	...
$(1s^2 2s^2_{1/2} 2p_{1/2} 2p^2_{3/2} 3s_{1/2})_4 \rightarrow (1s^2 2s^2_{1/2} 2p^2_{1/2} 2p^2_{3/2})_4$	5	57.322	IX-17	8	56.986	0.003	0.336	...	...	...
$(1s^2 2s^2_{1/2} 2p_{1/2} 2p^2_{3/2} 3s_{1/2})_4 \rightarrow (1s^2 2s^2_{1/2} 2p_{1/2} 2p^3_{3/2})_2$	1	57.564	IX-18	3	57.218	0.001	0.346	...	...	...
$(1s^2 2s_{1/2} 2p^2_{1/2} 2p^2_{3/2} 3s_{1/2})_4 \rightarrow (1s^2 2s_{1/2} 2p^2_{1/2} 2p^3_{3/2})_4$	5	57.991	IX-19	3 [e]	57.583	0.004	0.408	...	...	blend of 2 predicted lines
$(1s^2 2s_{1/2} 2p^2_{1/2} 2p^2_{3/2} 3s_{1/2})_4 \rightarrow (1s^2 2s_{1/2} 2p_{1/2} 2p^4_{3/2})_2$	2	58.219	IX-19	3 [e]	57.583	0.004	0.636	...	...	blend of 2 predicted lines
...	...	...	IX-20	2	58.851	0.006	...	...	...	...
$(1s^2 2s^2_{1/2} 2p^2_{1/2} 2p_{3/2} 3p_{3/2})_4 \rightarrow (1s^2 2s_{1/2} 2p^2_{1/2} 2p^3_{3/2})_4$	1	64.181	...	...	...	...	...	...	...	...
$(1s^2 2s^2_{1/2} 2p_{1/2} 2p^2_{3/2} 3p_{3/2})_4 \rightarrow (1s^2 2s_{1/2} 2p^2_{1/2} 2p^3_{3/2})_4$	4	65.118	IX-21	2	64.697	0.004	0.421	...	...	...
$(1s^2 2s^2_{1/2} 2p_{1/2} 2p^2_{3/2} 3p_{3/2})_4 \rightarrow (1s^2 2s_{1/2} 2p_{1/2} 2p^4_{3/2})_2$	1	65.405	IX-22	2	64.926	0.010	0.479	...	...	...

[a] Relative to strongest peak, scale 1–20

[b] $\lambda_{HULLAC} - \lambda_{EBIT}$

[c] Kaastra & Mewe 1993; Mewe, Kaastra, & Liedahl 1995

[d] $\lambda_{MEKAL} - \lambda_{EBIT}$

[e] Combined intensity of blended feature

Table 4. Summary of S X emission data.

HULLAC Transition	HULLAC Intensity [a]	HULLAC λ (Å)	Feature	Measured Intensity [a]	Measured λ (Å)	St. Error	Δλ [b]	MEKAL λ (Å) [c]	Δλ [d]	CHIANTI λ (Å) [e]	Comm
$(1s^22s^2_{1/2}2p_{1/2}2p_{3/2}5d_{5/2})_{3/2} \rightarrow (1s^22s^2_{1/2}2p_{1/2}2p^2_{3/2})_{3/2}$	1	31.596	X-1	6	31.511	0.007	0.085	...	...	...	..
$(1s^22p^4_{3/2}4d_{5/2})_{5/2} \rightarrow (1s^22s^2_{1/2}2p_{1/2}2p^2_{3/2})_{3/2}$	1	31.606	...	...	...	...	...	...	...	...	..
$(1s^22s_{1/2}2p^2_{1/2}2p_{3/2}4p_{1/2})_{5/2} \rightarrow (1s^22s^2_{1/2}2p_{1/2}2p^2_{3/2})_{3/2}$	1	32.933	X-2	1	32.407	0.007	0.526	...	...	...	..
$(1s^22s^2_{1/2}2p^2_{3/2}4d_{5/2})_{1/2} \rightarrow (1s^22s^2_{1/2}2p_{1/2}2p^2_{3/2})_{3/2}$	1	34.377	X-3	6 [f]	34.319	0.003	0.058	...	...	...	blend of 3 pre
$(1s^22s^2_{1/2}2p^2_{3/2}4d_{3/2})_{3/2} \rightarrow (1s^22s^2_{1/2}2p_{1/2}2p^2_{3/2})_{3/2}$	2	34.388	X-3	6 [f]	34.319	0.003	0.069	...	...	...	blend of 3 pre
$(1s^22s^2_{1/2}2p^2_{1/2}4d_{5/2})_{5/2} \rightarrow (1s^22s^2_{1/2}2p_{1/2}2p^2_{3/2})_{3/2}$	1	34.408	X-3	6 [f]	34.319	0.003	0.089	...	...	...	blend of 3 pre
$(1s^22s^2_{1/2}2p_{1/2}2p_{3/2}4d_{3/2})_{5/2} \rightarrow (1s^22s^2_{1/2}2p_{1/2}2p^2_{3/2})_{3/2}$	1	34.506	X-4	3	34.44	0.011	0.066	...	...	...	..
$(1s^22s^2_{1/2}2p_{1/2}2p_{3/2}4d_{3/2})_{5/2} \rightarrow (1s^22s^2_{1/2}2p^2_{1/2}2p_{3/2})_{3/2}$	1	34.767	X-5	6 [f]	34.623	0.009	0.144	...	...	...	blend of 2 predict
$(1s^22s^2_{1/2}2p_{1/2}2p_{3/2}4d_{3/2})_{7/2} \rightarrow (1s^22s^2_{1/2}2p_{1/2}2p^2_{3/2})_{5/2}$	1	34.792	X-5	6 [f]	34.623	0.009	0.169	...	...	...	blend of 2 predict
$(1s^22s^2_{1/2}2p^2_{3/2}4d_{5/2})_{7/2} \rightarrow (1s^22s^2_{1/2}2p_{1/2}2p^2_{3/2})_{5/2}$	1	35.411	X-6	1	35.278	0.006	0.133	...	...	...	..
$(1s^22s^2_{1/2}2p_{1/2}2p_{3/2}4d_{5/2})_{5/2} \rightarrow (1s^22s^2_{1/2}2p^2_{1/2}2p_{3/2})_{3/2}$	1	35.494	X-7	1	35.455	0.007	0.039	...	...	...	..
$(1s^22s^2_{1/2}2p^2_{3/2}4d_{3/2})_{5/2} \rightarrow (1s^22s^2_{1/2}2p^3_{3/2})_{3/2}$	< 1	35.849	X-8	1	35.756	0.006	0.093	...	...	...	..
...	...	...	X-9	1	35.996	0.003	...	...	...	...	..
$(1s^22s_{1/2}2p_{1/2}2p^2_{3/2}3p_{3/2})_{5/2} \rightarrow (1s^22s^2_{1/2}2p_{1/2}2p^2_{3/2})_{3/2}$	1	36.489	...	...	...	...	...	36.900	...	...	..
$(1s^22s_{1/2}2p^2_{1/2}2p_{3/2}3p_{3/2})_{3/2} \rightarrow (1s^22s^2_{1/2}2p^2_{1/2}2p_{3/2})_{3/2}$	1	39.711	...	...	...	...	...	...	...	...	blend of 2 predicte
$(1s^22s_{1/2}2p_{1/2}2p^2_{3/2}3p_{3/2})_{5/2} \rightarrow (1s^22s^2_{1/2}2p_{1/2}2p^2_{3/2})_{5/2}$	1	39.741	...	...	...	...	...	...	...	...	blend of 2 predicte
$(1s^22s_{1/2}2p^2_{1/2}2p_{3/2}3p_{3/2})_{5/2} \rightarrow (1s^22s^2_{1/2}2p^2_{1/2}2p_{3/2})_{3/2}$	1	40.278	X-10	1 [f]	40.211	0.0098	0.067	...	...	...	blend of 2 pre
$(1s^22s_{1/2}2p_{1/2}2p^2_{3/2}3p_{1/2})_{7/2} \rightarrow (1s^22s^2_{1/2}2p_{1/2}2p^2_{3/2})_{5/2}$	1	40.311	X-10	1 [f]	40.211	0.0098	0.100	...	...	...	blend of 2 pre
$(1s^22s_{1/2}2p^2_{1/2}2p_{3/2}3p_{3/2})_{1/2} \rightarrow (1s^22s^2_{1/2}2p_{1/2}2p^2_{3/2})_{3/2}$	1	41.545	X-11	9 [f]	41.363	0.022	0.182	...	...	...	blend of 3 predict
$(1s^22s_{1/2}2p^2_{1/2}2p_{3/2}3p_{1/2})_{3/2} \rightarrow (1s^22s^2_{1/2}2p_{1/2}2p^2_{3/2})_{3/2}$	2	41.551	X-11	9 [f]	41.363	0.022	0.188	...	...	...	blend of 3 predict
$(1s^22s_{1/2}2p_{1/2}2p^2_{3/2}3p_{1/2})_{5/2} \rightarrow (1s^22s^2_{1/2}2p_{1/2}2p^2_{3/2})_{3/2}$	2	41.558	X-11	9	41.363	0.022	0.195	...	...	...	blend of 3 predict
$(1s^22s^2_{1/2}2p^2_{3/2}3d_{3/2})_{1/2} \rightarrow (1s^22s^2_{1/2}2p_{1/2}2p^2_{3/2})_{3/2}$	7	42.581	...	...	...	...	...	...	...	42.5430	carbon
$(1s^22s^2_{1/2}2p^2_{3/2}3d_{3/2})_{3/2} \rightarrow (1s^22s^2_{1/2}2p_{1/2}2p^2_{3/2})_{3/2}$	14	42.605	...	...	...	...	...	...	...	...	carbon
$(1s^22s^2_{1/2}2p^2_{1/2}3d_{5/2})_{5/2} \rightarrow (1s^22s^2_{1/2}2p_{1/2}2p^2_{3/2})_{3/2}$	20	42.653	...	...	...	...	...	42.530	...	...	carbon
$(1s^22s^2_{1/2}2p^2_{3/2}3d_{3/2})_{3/2} \rightarrow (1s^22s^2_{1/2}2p_{1/2}2p^2_{3/2})_{1/2}$	1	42.768	...	...	...	...	...	...	...	...	carbon
$(1s^22s^2_{1/2}2p^2_{3/2}3d_{5/2})_{5/2} \rightarrow (1s^22s^2_{1/2}2p^3_{3/2})_{3/2}$	2	42.846	...	...	...	...	...	...	...	...	carbon
$(1s^22s^2_{1/2}2p^2_{3/2}3d_{3/2})_{5/2} \rightarrow (1s^22s^2_{1/2}2p_{1/2}2p^2_{3/2})_{3/2}$	2	42.917	...	...	...	...	...	...	...	...	carbon
$(1s^22s^2_{1/2}2p^2_{3/2}3d_{5/2})_{5/2} \rightarrow (1s^22s^2_{1/2}2p^2_{1/2}2p_{3/2})_{3/2}$	5	43.019	...	...	...	...	...	...	...	...	carbon
$(1s^22s^2_{1/2}2p_{1/2}2p_{3/2}3d_{5/2})_{7/2} \rightarrow (1s^22s^2_{1/2}2p_{1/2}2p^2_{3/2})_{5/2}$	10	43.097	...	...	...	...	...	43.002	...	...	carbon
$(1s^22s^2_{1/2}2p_{1/2}2p_{3/2}3d_{3/2})_{5/2} \rightarrow (1s^22s^2_{1/2}2p^2_{1/2}2p_{3/2})_{3/2}$	1	43.147	...	...	...	...	...	...	...	...	carbon
$(1s^22s^2_{1/2}2p_{1/2}2p_{3/2}3d_{3/2})_{3/2} \rightarrow (1s^22s^2_{1/2}2p^2_{1/2}2p_{3/2})_{3/2}$	1	43.175	...	...	...	...	...	...	...	...	carbon
$(1s^22s^2_{1/2}2p_{1/2}2p_{3/2}3d_{3/2})_{5/2} \rightarrow (1s^22s^2_{1/2}2p_{1/2}2p^2_{3/2})_{5/2}$	2	43.176	...	...	...	...	...	...	...	...	carbon
$(1s^22s^2_{1/2}2p_{1/2}2p_{3/2}3d_{3/2})_{7/2} \rightarrow (1s^22s^2_{1/2}2p_{1/2}2p^2_{3/2})_{5/2}$	1	43.352	...	...	...	...	...	...	...	...	carbon
$(1s^22s^2_{1/2}2p_{1/2}2p_{3/2}3d_{5/2})_{3/2} \rightarrow (1s^22s^2_{1/2}2p^3_{3/2})_{3/2}$	1	43.650	X-12	8 [f]	43.544	0.002	0.106	...	...	...	blend of 5 pre
$(1s^22s^2_{1/2}2p_{1/2}2p_{3/2}3d_{5/2})_{5/2} \rightarrow (1s^22s^2_{1/2}2p^2_{1/2}2p_{3/2})_{3/2}$	1	43.658	X-12	8 [f]	43.544	0.002	0.114	...	...	...	blend of 5 pre
$(1s^22s^2_{1/2}2p_{1/2}2p_{3/2}3d_{3/2})_{1/2} \rightarrow (1s^22s^2_{1/2}2p_{1/2}2p^2_{3/2})_{1/2}$	1	43.66	X-12	8 [f]	43.544	0.002	0.116	...	...	...	blend of 5 pre
$(1s^22s^2_{1/2}2p_{1/2}2p_{3/2}3d_{5/2})_{5/2} \rightarrow (1s^22s^2_{1/2}2p_{1/2}2p^2_{3/2})_{5/2}$	2	43.688	X-12	8 [f]	43.544	0.002	0.144	...	...	...	blend of 5 pre
$(1s^22s^2_{1/2}2p^2_{3/2}3d_{5/2})_{3/2} \rightarrow (1s^22s^2_{1/2}2p^2_{1/2}2p_{3/2})_{3/2}$	1	43.692	X-12	8 [f]	43.544	0.002	0.148	...	...	...	blend of 5 pre
$(1s^22s^2_{1/2}2p^2_{3/2}3d_{5/2})_{5/2} \rightarrow (1s^22s^2_{1/2}2p^3_{3/2})_{3/2}$	2	43.842	X-13	5	43.765	0.011	0.077	...	...	...	..
$(1s^22s^2_{1/2}2p_{1/2}2p_{3/2}3d_{3/2})_{3/2} \rightarrow (1s^22s^2_{1/2}2p_{1/2}2p^2_{3/2})_{1/2}$	1	43.964	X-14	6	43.859	0.011	0.105	...	...	...	..
$(1s^22s^2_{1/2}2p^2_{3/2}3d_{3/2})_{5/2} \rightarrow (1s^22s^2_{1/2}2p^3_{3/2})_{3/2}$	2	43.975	X-14	6	43.859	0.011	0.116	...	...	...	..
$(1s^22s^2_{1/2}2p^2_{3/2}3d_{5/2})_{7/2} \rightarrow (1s^22s^2_{1/2}2p_{1/2}2p^2_{3/2})_{5/2}$	2	44.259	X-15	2	44.093	0.002	0.166	...	...	...	..
$(1s^22s^2_{1/2}2p_{1/2}2p_{3/2}3d_{5/2})_{5/2} \rightarrow (1s^22s^2_{1/2}2p^2_{1/2}2p_{3/2})_{3/2}$	2	44.397	X-16	10 [f]	44.386	0.002	0.011	...	...	...	blend of 3 predicted
$(1s^22s^2_{1/2}2p^2_{3/2}3d_{5/2})_{3/2} \rightarrow (1s^22s^2_{1/2}2p_{1/2}2p^2_{3/2})_{1/2}$	1	44.501	X-16	10 [f]	44.386	0.002	0.115	...	...	...	blend of 3 predicted
$(1s^22s^2_{1/2}2p_{1/2}2p_{3/2}3d_{5/2})_{5/2} \rightarrow (1s^22s^2_{1/2}2p^3_{3/2})_{3/2}$	1	44.506	X-16	10 [f]	44.386	0.002	0.120	...	...	...	blend of 3 predicted
$(1s^22s^2_{1/2}2p_{1/2}2p_{3/2}3d_{5/2})_{7/2} \rightarrow (1s^22s^2_{1/2}2p_{1/2}2p^2_{3/2})_{5/2}$	1	44.851	X-17	4	44.565	0.006	0.286	...	...	...	blend w
$(1s^22s_{1/2}2p_{1/2}2p^2_{3/2}3d_{5/2})_{7/2} \rightarrow (1s^22s_{1/2}2p_{1/2}2p^3_{3/2})_{5/2}$	1	45.536	X-18	8 [f]	45.287	0.004	0.249	...	...	...	blend of 2 predicted

Table 4—Continued

HULLAC Transition	HULLAC Intensity [a]	HULLAC λ (Å)	Feature	Measured Intensity [a]	Measured λ (Å)	St. Error	$\Delta\lambda$ [b]	MEKAL λ (Å) [c]	$\Delta\lambda$ [d]	CHIANTI λ (Å) [e]	Comm
$(1s^2 2s^2_{1/2} 2p^2_{3/2} 3s_{1/2})_{5/2} \rightarrow (1s^2 2s^2_{1/2} 2p_{1/2} 2p^2_{3/2})_{3/2}$	6	47.818	X-20	20	47.637	0.004	0.181	47.694	0.057	...	..
$(1s^2 2s^2_{1/2} 2p_{1/2} 2p_{3/2} 3s_{1/2})_{3/2} \rightarrow (1s^2 2s^2_{1/2} 2p_{1/2} 2p^2_{3/2})_{3/2}$	3	47.969	X-21	15 [f]	47.809	0.009	0.160	47.793	-0.016	...	blend of 2 predict
$(1s^2 2s^2_{1/2} 2p^2_{1/2} 3s_{1/2})_{1/2} \rightarrow (1s^2 2s^2_{1/2} 2p_{1/2} 2p^2_{3/2})_{3/2}$	2	48.07	X-21	15 [f]	47.809	0.009	0.261	47.793	-0.016	...	blend of 2 predict
$(1s^2 2s^2_{1/2} 2p_{1/2} 2p_{3/2} 3s_{1/2})_{3/2} \rightarrow (1s^2 2s^2_{1/2} 2p^2_{1/2} 2p_{3/2})_{3/2}$	1	48.336	X-22	9 [f]	48.158	0.002	0.178	...	...	...	blend of 2 predict
$(1s^2 2s^2_{1/2} 2p_{1/2} 2p_{3/2} 3s_{1/2})_{5/2} \rightarrow (1s^2 2s^2_{1/2} 2p_{1/2} 2p^2_{3/2})_{5/2}$	2	48.379	X-22	9 [f]	48.158	0.002	0.221	...	...	...	blend of 2 predict
$(1s^2 2s^2_{1/2} 2p^2_{3/2} 3s_{1/2})_{3/2} \rightarrow (1s^2 2s^2_{1/2} 2p_{1/2} 2p^2_{3/2})_{5/2}$	2	49.354	...	...	49.127	0.003	0.227	...	...	...	blend of 2 predicte
$(1s^2 2s^2_{1/2} 2p_{1/2} 2p_{3/2} 3s_{1/2})_{5/2} \rightarrow (1s^2 2s^2_{1/2} 2p^3_{3/2})_{3/2}$	1	49.385	...	...	49.127	0.003	0.258	...	...	...	blend of 2 predicte
$(1s^2 2s^2_{1/2} 2p_{1/2} 2p_{3/2} 3s_{1/2})_{1/2} \rightarrow (1s^2 2s^2_{1/2} 2p^2_{1/2} 2p_{3/2})_{3/2}$	1	49.506	X-23	5	49.326	0.004	0.180	...	...	...	blend w
$(1s^2 2s^2_{1/2} 2p^2_{3/2} 3s_{1/2})_{3/2} \rightarrow (1s^2 2s^2_{1/2} 2p^3_{3/2})_{3/2}$	1	50.401	X-24	2	50.398	0.006	0.003	...	...	...	..
$(1s^2 2s_{1/2} 2p_{1/2} 2p^2_{3/2} 3s_{1/2})_{3/2} \rightarrow (1s^2 2s_{1/2} 2p_{1/2} 2p^3_{3/2})_{3/2}$	1	51.239	X-25	5 [f]	51.132	0.005	0.107	...	...	...	blend of 2 pr
$(1s^2 2s_{1/2} 2p_{1/2} 2p^2_{3/2} 3s_{1/2})_{5/2} \rightarrow (1s^2 2s_{1/2} 2p_{1/2} 2p^3_{3/2})_{5/2}$	2	51.243	X-25	5 [f]	51.132	0.005	0.111	...	...	...	blend of 2 pr
$(1s^2 2s_{1/2} 2p^2_{1/2} 2p_{3/2} 3s_{1/2})_{3/2} \rightarrow (1s^2 2s_{1/2} 2p^2_{1/2} 2p^2_{3/2})_{5/2}$	4	51.378	X-26	2	51.277	0.008	0.101	...	...	...	..
$(1s^2 2s_{1/2} 2p_{1/2} 2p^2_{3/2} 3p_{1/2})_{5/2} \rightarrow (1s^2 2s^2_{1/2} 2p_{1/2} 2p^2_{3/2})_{3/2}$	2	51.544	X-27	3 [f]	51.434	0.014	0.110	...	...	...	blend of 2 pr
$(1s^2 2s_{1/2} 2p^2_{1/2} 2p_{3/2} 3s_{1/2})_{3/2} \rightarrow (1s^2 2s_{1/2} 2p^4_{3/2})_{1/2}$	1	51.64	X-27	3 [f]	51.434	0.014	0.206	...	...	...	blend of 2 pr
$(1s^2 2s_{1/2} 2p^2_{1/2} 2p_{3/2} 3s_{1/2})_{5/2} \rightarrow (1s^2 2s_{1/2} 2p^2_{1/2} 2p^2_{3/2})_{5/2}$	1	53.218	...	...	...	...	...	...	...	...	blend of 2 predict
$(1s^2 2s^2_{1/2} 2p_{1/2} 2p_{3/2} 3s_{1/2})_{3/2} \rightarrow (1s^2 2s_{1/2} 2p^2_{1/2} 2p^2_{3/2})_{5/2}$	2	54.302	...	...	...	...	...	...	...	...	blend of 2 predict
$(1s^2 2s^2_{1/2} 2p_{1/2} 2p_{3/2} 3s_{1/2})_{3/2} \rightarrow (1s^2 2s_{1/2} 2p_{1/2} 2p^3_{3/2})_{3/2}$	2	54.489	...	...	...	...	...	...	...	...	blend of 2 predic
$(1s^2 2s^2_{1/2} 2p_{1/2} 2p_{3/2} 3p_{3/2})_{3/2} \rightarrow (1s^2 2s_{1/2} 2p^4_{3/2})_{1/2}$	1	54.596	...	...	...	...	...	...	...	...	blend of 2 predic
$(1s^2 2s^2_{1/2} 2p_{1/2} 2p_{3/2} 3p_{1/2})_{5/2} \rightarrow (1s^2 2s_{1/2} 2p^2_{1/2} 2p^2_{3/2})_{5/2}$	1	54.816	...	...	...	...	...	...	...	...	blend w
$(1s^2 2s^2_{1/2} 2p^2_{1/2} 3p_{3/2})_{3/2} \rightarrow (1s^2 2s_{1/2} 2p^2_{1/2} 2p^2_{3/2})_{5/2}$	1	54.934	X-28	1	54.765	0.017	0.169	...	...	...	..
$(1s^2 2s^2_{1/2} 2p_{1/2} 2p_{3/2} 3p_{3/2})_{5/2} \rightarrow (1s^2 2s_{1/2} 2p_{1/2} 2p^3_{3/2})_{5/2}$	1	57.016	X-29	3 [f]	56.548	0.006	0.468	...	...	...	blend of 2 pr
$(1s^2 2s^2_{1/2} 2p_{1/2} 2p_{3/2} 3p_{1/2})_{3/2} \rightarrow (1s^2 2s_{1/2} 2p_{1/2} 2p^3_{3/2})_{3/2}$	1	57.017	X-29	3 [f]	56.548	0.006	0.469	...	...	...	blend of 2 pr

[a] Relative to strongest peak, scale 1–20

[b] $\lambda_{HULLAC} - \lambda_{EBIT}$

[c] Kaastra & Mewe 1993; Mewe, Kaastra, & Liedahl 1995

[d] $\lambda_{MEKAL} - \lambda_{EBIT}$

[e] Dere et al. 1997, 2001

[f] Combined intensity of blended feature

Table 5. Summary of S XI emission data.

HULLAC Transition	HULLAC Intensity [a]	HULLAC λ (Å)	Feature	Measured Intensity [a]	Measured λ (Å)	St. Error	Δλ [b]	MEKAL λ (Å) [c]	Δλ [d]	Comment
$(1s^22s^2_{1/2}2p_{3/2}5d_{5/2})_6 \rightarrow (1s^22s^2_{1/2}2p^2_{3/2})_4$	1	28.404	XI-1	3	28.315	0.005	0.089	...	...	...
$(1s^22s_{1/2}2p^2_{3/2}4p_{3/2})_6 \rightarrow (1s^22s^2_{1/2}2p^2_{3/2})_4$	< 1	29.684	XI-2	2	29.549	0.003	0.135	...	...	...
$(1s^22s^2_{1/2}2p_{3/2}4d_{5/2})_4 \rightarrow (1s^22s^2_{1/2}2p_{1/2}2p_{3/2})_2$	1	31.106	XI-3	6 [e]	31.050	0.003	0.056	...	...	blend of 5 predicted lines
$(1s^22s^2_{1/2}2p_{1/2}4d_{3/2})_2 \rightarrow (1s^22s^2_{1/2}2p^2_{1/2})_0$	1	31.108	XI-3	6 [e]	31.050	0.003	0.058	...	...	blend of 5 predicted lines
$(1s^22s^2_{1/2}2p_{3/2}4d_{3/2})_4 \rightarrow (1s^22s^2_{1/2}2p^2_{3/2})_4$	1	31.122	XI-3	6 [e]	31.050	0.003	0.072	...	...	blend of 5 predicted lines
$(1s^22s^2_{1/2}2p_{3/2}4d_{5/2})_6 \rightarrow (1s^22s^2_{1/2}2p^2_{3/2})_4$	2	31.144	XI-3	6 [e]	31.050	0.003	0.094	...	...	blend of 5 predicted lines
$(1s^22s^2_{1/2}2p_{1/2}4d_{5/2})_4 \rightarrow (1s^22s^2_{1/2}2p_{1/2}2p_{3/2})_2$	1	31.198	XI-3	6 [e]	31.050	0.003	0.148	...	...	blend of 5 predicted lines
$(1s^22s^2_{1/2}2p_{3/2}4d_{3/2})_6 \rightarrow (1s^22s^2_{1/2}2p_{1/2}2p_{3/2})_4$	1	31.584	...	2	31.511	0.007	0.073	...	...	blend w/ X-1
$(1s^22s_{1/2}2p^2_{3/2}3p_{3/2})_6 \rightarrow (1s^22s^2_{1/2}2p^2_{3/2})_4$	1	34.652	...	3	34.623	0.009	0.029	...	...	blend w/ X-5
$(1s^22s_{1/2}2p_{1/2}2p_{3/2}3p_{3/2})_6 \rightarrow (1s^22s^2_{1/2}2p_{1/2}2p_{3/2})_4$	1	36.803	...	...	...	...	...	...	...	...
$(1s^22s_{1/2}2p_{1/2}2p_{3/2}3p_{3/2})_4 \rightarrow (1s^22s^2_{1/2}2p^2_{3/2})_4$	2	37.723	XI-4	1 [e]	37.600	0.006	0.123	37.340	-0.260	blend of 2 predicted lines
$(1s^22s_{1/2}2p^2_{3/2}3p_{3/2})_2 \rightarrow (1s^22s^2_{1/2}2p^2_{3/2})_4$	1	37.756	XI-4	1 [e]	37.600	0.006	0.156	37.340	-0.260	blend of 2 predicted lines
$(1s^22s_{1/2}2p^2_{3/2}3d_{5/2})_8 \rightarrow (1s^22s_{1/2}2p_{1/2}2p^2_{3/2})_6$	1	37.833	XI-5	1 [e]	37.745	0.008	0.088	37.780	0.035	blend of 4 predicted lines
$(1s^22s_{1/2}2p_{1/2}2p_{3/2}3d_{5/2})_6 \rightarrow (1s^22s_{1/2}2p_{1/2}2p^2_{3/2})_4$	1	37.873	XI-5	1 [e]	37.745	0.008	0.128	37.780	0.035	blend of 4 predicted lines
$(1s^22s_{1/2}2p^2_{1/2}3p_{3/2})_4 \rightarrow (1s^22s^2_{1/2}2p_{1/2}2p_{3/2})_2$	2	37.910	XI-5	1 [e]	37.745	0.008	0.165	37.780	0.035	blend of 4 predicted lines
$(1s^22s_{1/2}2p^2_{3/2}3p_{3/2})_6 \rightarrow (1s^22s^2_{1/2}2p^2_{3/2})_4$	3	37.937	XI-5	1 [e]	37.745	0.008	0.192	37.780	0.035	blend of 4 predicted lines
$(1s^22s_{1/2}2p^2_{1/2}3p_{1/2})_2 \rightarrow (1s^22s^2_{1/2}2p^2_{3/2})_4$	1	38.731	...	...	...	...	...	...	...	...
$(1s^22s^2_{1/2}2p_{3/2}3d_{3/2})_0 \rightarrow (1s^22s^2_{1/2}2p_{1/2}2p_{3/2})_2$	2	39.202	XI-6	2 [e]	39.081	0.005	0.121	...	...	blend of 3 predicted lines
$(1s^22s^2_{1/2}2p_{3/2}3d_{3/2})_2 \rightarrow (1s^22s^2_{1/2}2p_{1/2}2p_{3/2})_2$	3	39.215	XI-6	2 [e]	39.081	0.005	0.134	...	...	blend of 3 predicted lines
$(1s^22s_{1/2}2p_{1/2}2p_{3/2}3d_{3/2})_8 \rightarrow (1s^22s_{1/2}2p_{1/2}2p^2_{3/2})_6$	1	39.226	XI-7	2 [e]	39.081	0.005	0.145	...	...	blend of 3 predicted lines
$(1s^22s^2_{1/2}2p_{3/2}3d_{3/2})_2 \rightarrow (1s^22s^2_{1/2}2p^2_{3/2})_4$	2	39.331	XI-7	20 [e]	39.287	0.002	0.044	39.240	-0.047	blend of 6 predicted lines
$(1s^22s^2_{1/2}2p_{1/2}3d_{3/2})_2 \rightarrow (1s^22s^2_{1/2}2p^2_{1/2})_0$	7	39.342	XI-7	20 [e]	39.287	0.002	0.055	39.240	-0.047	blend of 6 predicted lines
$(1s^22s^2_{1/2}2p_{3/2}3d_{5/2})_4 \rightarrow (1s^22s^2_{1/2}2p^2_{3/2})_4$	9	39.354	XI-7	20 [e]	39.287	0.002	0.067	39.240	-0.047	blend of 6 predicted lines
$(1s^22s^2_{1/2}2p_{3/2}3d_{5/2})_4 \rightarrow (1s^22s^2_{1/2}2p_{1/2}2p_{3/2})_2$	13	39.388	XI-7	20 [e]	39.287	0.002	0.101	39.300	0.013	blend of 6 predicted lines
$(1s^22s^2_{1/2}2p_{1/2}3d_{3/2})_2 \rightarrow (1s^22s^2_{1/2}2p_{1/2}2p_{3/2})_2$	2	39.416	XI-7	20 [e]	39.287	0.002	0.129	39.300	0.013	blend of 6 predicted lines
$(1s^22s^2_{1/2}2p_{3/2}3d_{5/2})_6 \rightarrow (1s^22s^2_{1/2}2p^2_{3/2})_4$	20	39.427	XI-7	20 [e]	39.287	0.002	0.140	39.300	0.013	blend of 6 predicted lines
$(1s^22s^2_{1/2}2p_{3/2}3d_{3/2})_6 \rightarrow (1s^22s^2_{1/2}2p_{1/2}2p_{3/2})_4$	8	39.735	XI-8	4 [e]	39.671	0.003	0.064	...	...	blend of 2 predicted lines
$(1s^22s^2_{1/2}2p_{1/2}3d_{5/2})_6 \rightarrow (1s^22s^2_{1/2}2p^2_{3/2})_4$	1	39.824	XI-8	4 [e]	39.671	0.003	0.153	...	...	blend of 2 predicted lines
$(1s^22s_{1/2}2p^2_{3/2}3d_{5/2})_4 \rightarrow (1s^22s_{1/2}2p_{1/2}2p^2_{3/2})_2$	1	40.359	...	...	...	...	...	...	...	...
$(1s^22s^2_{1/2}2p_{3/2}3d_{3/2})_4 \rightarrow (1s^22s^2_{1/2}2p_{1/2}2p_{3/2})_4$	2	40.747	...	...	...	...	...	...	...	...
$(1s^22s^2_{1/2}2p_{3/2}3d_{5/2})_2 \rightarrow (1s^22s^2_{1/2}2p^2_{3/2})_0$	1	40.773	...	...	...	...	...	...	...	...
$(1s^22s^2_{1/2}2p_{1/2}3d_{3/2})_4 \rightarrow (1s^22s^2_{1/2}2p_{1/2}2p_{3/2})_4$	1	40.885	...	...	...	...	...	...	...	...
$(1s^22s_{1/2}2p^2_{3/2}3d_{5/2})_6 \rightarrow (1s^22s_{1/2}2p_{1/2}2p^2_{3/2})_6$	1	41.108	...	...	...	...	...	...	...	...
$(1s^22s_{1/2}2p^2_{3/2}3d_{5/2})_8 \rightarrow (1s^22s_{1/2}2p_{1/2}2p^2_{3/2})_6$	2	41.577	...	...	...	...	...	...	...	...
$(1s^22s_{1/2}2p^2_{3/2}3d_{3/2})_6 \rightarrow (1s^22s_{1/2}2p_{1/2}2p^2_{3/2})_4$	2	41.661	...	...	...	...	...	...	...	...
$(1s^22s_{1/2}2p_{1/2}2p_{3/2}3d_{5/2})_4 \rightarrow (1s^22s_{1/2}2p^2_{1/2}2p_{3/2})_2$	1	41.733	...	...	...	...	...	...	...	...
$(1s^22s_{1/2}2p^2_{3/2}3d_{5/2})_6 \rightarrow (1s^22s_{1/2}2p^3_{3/2})_4$	1	42.193	...	...	...	...	...	...	...	...
$(1s^22s_{1/2}2p_{1/2}2p_{3/2}3d_{5/2})_6 \rightarrow (1s^22s_{1/2}2p_{1/2}2p^2_{3/2})_4$	1	42.618	...	...	...	...	...	...	...	...
$(1s^22s^2_{1/2}2p_{3/2}3s_{1/2})_4 \rightarrow (1s^22s^2_{1/2}2p_{1/2}2p_{3/2})_2$	1	43.164	...	...	...	...	...	...	...	...
$(1s^22s^2_{1/2}2p_{1/2}3s_{1/2})_2 \rightarrow (1s^22s^2_{1/2}2p^2_{1/2})_0$	1	43.264	...	...	...	...	...	...	...	...
$(1s^22s^2_{1/2}2p_{3/2}3s_{1/2})_4 \rightarrow (1s^22s^2_{1/2}2p^2_{3/2})_4$	3	43.304	XI-9	3 [e]	43.298	0.003	0.006	...	...	blend of 3 predicted lines
$(1s^22s^2_{1/2}2p_{1/2}3s_{1/2})_0 \rightarrow (1s^22s^2_{1/2}2p_{1/2}2p_{3/2})_2$	1	43.406	XI-9	3 [e]	43.298	0.003	0.108	...	...	blend of 3 predicted lines
$(1s^22s^2_{1/2}2p_{1/2}3s_{1/2})_2 \rightarrow (1s^22s^2_{1/2}2p^2_{3/2})_4$	1	43.495	XI-9	3 [e]	43.298	0.003	0.197	...	...	blend of 3 predicted lines
$(1s^22s^2_{1/2}2p_{3/2}3s_{1/2})_2s \rightarrow (1s^22s^2_{1/2}2p_{1/2}2p_{3/2})_4$	1	44.112	...	...	...	...	...	...	...	...
$(1s^22s_{1/2}2p^2_{3/2}3s_{1/2})_4 \rightarrow (1s^22s_{1/2}2p_{1/2}2p^2_{3/2})_6$	3	45.258	XI-10	2	45.008	0.006	0.250	...	...	...
$(1s^22s_{1/2}2p_{1/2}2p_{3/2}3s_{1/2})_2 \rightarrow (1s^22s_{1/2}2p_{1/2}2p^2_{3/2})_4$	2	45.387	XI-11	2 [e]	45.124	0.007	0.263	...	...	blend of 2 predicted lines
$(1s^22s_{1/2}2p_{1/2}2p_{3/2}3s_{1/2})_0 \rightarrow (1s^22s_{1/2}2p^2_{1/2}2p_{3/2})_2$	1	45.465	XI-11	2 [e]	45.124	0.007	0.341	...	...	blend of 2 predicted lines

Table 5—Continued

HULLAC Transition	HULLAC Intensity [a]	HULLAC λ (Å)	Feature	Measured Intensity [a]	Measured λ (Å)	St. Error	$\Delta\lambda$ [b]	MEKAL λ (Å) [c]	$\Delta\lambda$ [d]	Comment
$(1s^2 2s^2_{1/2} 2p_{3/2} 3p_{1/2})_2 \rightarrow (1s^2 2s_{1/2} 2p_{1/2} 2p^2_{3/2})_4$	1	48.108	XI-12	3 [e]	48.158	0.002	-0.050	...	...	blend of 3 predicted lines, w/ IX-9
$(1s^2 2s^2_{1/2} 2p_{1/2} 3p_{1/2})_0 \rightarrow (1s^2 2s_{1/2} 2p^2_{1/2} 2p_{3/2})_2$	1	48.238	XI-12	3 [e]	48.158	0.002	0.080	...	...	blend of 3 predicted lines, w/ IX-9
...	...	...	XI-13	3	49.714	0.007	...	...	...	...
$(1s^2 2s^2_{1/2} 2p_{3/2} 3p_{3/2})_6 \rightarrow (1s^2 2s_{1/2} 2p^3_{3/2})_4$	1	49.991	XI-14	2	49.981	0.008	0.010	...	...	...
$(1s^2 2s^2_{1/2} 2p_{3/2} 3p_{3/2})_4 \rightarrow (1s^2 2s_{1/2} 2p_{1/2} 2p^2_{3/2})_4$	1	52.004	...	...	...	...	...	...	...	blend w/ VII

[a] Relative to strongest peak, scale 1–20

[b] $\lambda_{HULLAC} - \lambda_{EBIT}$

[c] Kaastra & Mewe 1993; Mewe, Kaastra, & Liedahl 1995

[d] $\lambda_{MEKAL} - \lambda_{EBIT}$

[e] Combined intensity of blended feature

Table 6. Summary of S XII emission data.

HULLAC Transition	HULLAC Intensity [a]	HULLAC λ (Å)	Feature	Measured Intensity [a]	Measured λ (Å)	St. Error	$\Delta\lambda$ [b]	MEKAL λ (Å) [c]	$\Delta\lambda$ [d]	CHIANTI λ (Å) [e]	$\Delta\lambda$ [f]	Co
$(1s^22s^2_{1/2}5d_{3/2})_{3/2} \rightarrow (1s^22s^2_{1/2}2p_{1/2})_{1/2}$	1	25.645	XII-1	4 [g]	25.658	0.014	-0.013	...	...	...	...	blend of 2
$(1s^22s^2_{1/2}5d_{5/2})_{5/2} \rightarrow (1s^22s^2_{1/2}2p_{3/2})_{3/2}$	1	25.728	XII-1	4 [g]	25.658	0.014	0.070	...	...	...	...	blend of 2
$(1s^22s_{1/2}2p_{3/2}4p_{3/2})_{5/2} \rightarrow (1s^22s^2_{1/2}2p_{3/2})_{3/2}$	1	26.907	...	...	...	...	...	27.800	...	...	...	blend domi
$(1s^22s^2_{1/2}4d_{3/2})_{3/2} \rightarrow (1s^22s^2_{1/2}2p_{1/2})_{1/2}$	2	28.282	...	5 [g]	28.315	0.005	-0.033	...	...	...	...	blend of 2 predic
$(1s^22s^2_{1/2}4d_{5/2})_{5/2} \rightarrow (1s^22s^2_{1/2}2p_{3/2})_{3/2}$	3	28.383	...	5 [g]	28.315	0.005	0.068	...	...	...	...	blend of 2 predic
$(1s^22s_{1/2}2p_{3/2}3p_{3/2})_{5/2} \rightarrow (1s^22s^2_{1/2}2p_{3/2})_{3/2}$	1	32.871	XII-2	3 [g]	32.899	0.004	-0.028	...	...	...	...	blend of 2
$(1s^22s_{1/2}2p_{3/2}3p_{1/2})_{3/2} \rightarrow (1s^22s^2_{1/2}2p_{3/2})_{3/2}$	1	32.896	XII-2	3 [g]	32.899	0.004	-0.003	...	...	...	...	blend of 2
$(1s^22s_{1/2}2p_{3/2}3p_{3/2})_{1/2} \rightarrow (1s^22s^2_{1/2}2p_{3/2})_{3/2}$	1	34.350	...	...	...	...	...	...	...	...	...	blend dor
$(1s^22s_{1/2}2p_{1/2}3p_{3/2})_{3/2} \rightarrow (1s^22s^2_{1/2}2p_{1/2})_{1/2}$	3	34.601	...	8 [g]	34.592	0.001	0.009	...	...	...	...	blend of 3 predict
$(1s^22s_{1/2}2p_{3/2}3p_{3/2})_{5/2} \rightarrow (1s^22s^2_{1/2}2p_{3/2})_{3/2}$	5	34.655	...	8 [g]	34.592	0.001	0.063	...	...	...	...	blend of 3 predict
$(1s^22s_{1/2}2p_{1/2}3p_{3/2})_{3/2} \rightarrow (1s^22s^2_{1/2}2p_{3/2})_{3/2}$	1	34.757	...	8 [g]	34.592	0.001	0.165	...	...	...	...	blend of 3 predict
$(1s^22s_{1/2}2p_{1/2}3p_{3/2})_{1/2} \rightarrow (1s^22s^2_{1/2}2p_{1/2})_{1/2}$	1	35.158	XII-3	3 [g]	35.221	0.006	-0.063	...	...	...	...	blend of 3 predict
$(1s^22s_{1/2}2p_{1/2}3p_{3/2})_{3/2} \rightarrow (1s^22s^2_{1/2}2p_{3/2})_{3/2}$	2	35.298	XII-3	3 [g]	35.221	0.006	0.077	...	...	...	...	blend of 3 predict
$(1s^22s_{1/2}2p_{1/2}3p_{1/2})_{3/2} \rightarrow (1s^22s^2_{1/2}2p_{3/2})_{3/2}$	1	35.369	XII-3	3 [g]	35.221	0.006	0.148	...	...	...	...	blend of 3 predict
$(1s^22s_{1/2}2p_{3/2}3d_{5/2})_{7/2} \rightarrow (1s^22s_{1/2}2p_{1/2}2p_{3/2})_{5/2}$	1	35.932	XII-4	2	35.968	0.001	-0.036	...	...	...	...	blen
$(1s^22s_{1/2}2p_{3/2}3d_{3/2})_{5/2} \rightarrow (1s^22s_{1/2}2p_{1/2}2p_{3/2})_{3/2}$	1	36.245	XII-5	13 [g]	36.397	0.003	-0.152	36.398	0.001	36.3980	0.001	blend of 2
$(1s^22s^2_{1/2}3d_{3/2})_{3/2} \rightarrow (1s^22s^2_{1/2}2p_{1/2})_{1/2}$	12	36.488	XII-5	13 [g]	36.397	0.003	0.091	36.398	0.001	36.3980	0.001	blend of 2
$(1s^22s^2_{1/2}3d_{5/2})_{5/2} \rightarrow (1s^22s^2_{1/2}2p_{3/2})_{3/2}$	20	36.649	XII-6	20 [g]	36.564	0.003	0.085	36.563	-0.001	36.5640	0.000	blend of 2
$(1s^22s^2_{1/2}3d_{3/2})_{3/2} \rightarrow (1s^22s^2_{1/2}2p_{3/2})_{3/2}$	2	36.662	XII-6	20 [g]	36.564	0.003	0.098	36.563	-0.001	36.5730	0.009	blend of 2
$(1s^22s_{1/2}2p_{3/2}3d_{3/2})_{3/2} \rightarrow (1s^22s_{1/2}2p_{1/2}2p_{3/2})_{1/2}$	1	37.496	...	...	...	...	...	...	...	...	...	blend domi
$(1s^22s_{1/2}2p_{3/2}3d_{5/2})_{5/2} \rightarrow (1s^22s_{1/2}2p^2_{3/2})_{3/2}$	1	37.58	...	...	...	...	...	...	...	...	...	blend domi
$(1s^22s_{1/2}2p_{3/2}3d_{3/2})_{7/2} \rightarrow (1s^22s_{1/2}2p_{1/2}2p_{3/2})_{5/2}$	4	37.722	...	...	...	...	...	...	...	37.715	...	blen
$(1s^22s_{1/2}2p_{1/2}3d_{5/2})_{5/2} \rightarrow (1s^22s_{1/2}2p_{1/2}2p_{3/2})_{3/2}$	3	37.836	...	...	...	...	...	...	...	...	...	blen
$(1s^22s_{1/2}2p_{1/2}3d_{1/2})_{3/2} \rightarrow (1s^22s_{1/2}2p_{1/2}2p_{3/2})_{3/2}$	1	38.546	XII-7	2	38.326	0.008	0.220	...	...	...	...	
$(1s^22s_{1/2}2p_{3/2}3d_{5/2})_{1/2} \rightarrow (1s^22s_{1/2}2p^2_{3/2})_{1/2}$	1	39.026	XII-8	5 [g]	38.900	0.005	0.126	...	...	...	...	blend of 2
$(1s^22s_{1/2}2p_{3/2}3d_{5/2})_{3/2} \rightarrow (1s^22s_{1/2}2p^2_{3/2})_{1/2}$	2	39.096	XII-8	5 [g]	38.900	0.005	0.196	...	...	...	...	blend of 2
$(1s^22s^2_{1/2}3s_{1/2})_{1/2} \rightarrow (1s^22s^2_{1/2}2p_{1/2})_{1/2}$	1	39.252	...	...	...	...	...	...	...	...	...	blend dom
$(1s^22s^2_{1/2}3s_{1/2})_{1/2} \rightarrow (1s^22s^2_{1/2}2p_{3/2})_{3/2}$	2	39.452	...	...	...	...	...	...	...	...	...	blend dom
$(1s^22s_{1/2}2p_{3/2}3s_{1/2})_{3/2} \rightarrow (1s^22s_{1/2}2p_{1/2}2p_{3/2})_{5/2}$	4	40.755	XII-9	6	40.543	0.008	0.212	...	...	...	...	
$(1s^22s_{1/2}2p_{1/2}3s_{1/2})_{1/2} \rightarrow (1s^22s_{1/2}2p_{1/2}2p_{3/2})_{5/2}$	2	40.898	...	...	...	...	...	...	...	...	...	
$(1s^22s_{1/2}2p_{3/2}3s_{1/2})_{3/2} \rightarrow (1s^22s_{1/2}2p^2_{3/2})_{1/2}$	1	42.378	...	...	...	...	...	...	...	...	...	carl
$(1s^22s_{1/2}2p_{1/2}3s_{1/2})_{1/2} \rightarrow (1s^22s_{1/2}2p^2_{3/2})_{1/2}$	1	42.538	...	...	...	...	...	...	...	...	...	carl
$(1s^22s^2_{1/2}3p_{3/2})_{3/2} \rightarrow (1s^22s_{1/2}2p_{1/2}2p_{3/2})_{5/2}$	3	43.574	...	...	...	...	...	...	...	...	...	blend dom
$(1s^22s^2_{1/2}3p_{1/2})_{1/2} \rightarrow (1s^22s_{1/2}2p_{1/2}2p_{3/2})_{3/2}$	2	43.635	...	...	...	...	...	...	...	...	...	blend dom

[a] Relative to strongest peak, scale 1–20

[b] $\lambda_{HULLAC} - \lambda_{EBIT}$

[c] Kaastra & Mewe 1993; Mewe, Kaastra, & Liedahl 1995

[d] $\lambda_{MEKAL} - \lambda_{EBIT}$

[e] Dere et al. 1997, 2001

[f] $\lambda_{CHIANTI} - \lambda_{EBIT}$

[g] Combined intensity of blended feature

Table 7. Summary of S XIII emission data.

HULLAC Transition	HULLAC Intensity [a]	HULLAC λ (Å)	Feature	Measured Intensity [a]	Measured λ (Å)	St. Error	$\Delta\lambda$ [b]	MEKAL λ (Å) [c]	$\Delta\lambda$ [d]	CHIANTI λ (Å) [e]	$\Delta\lambda$ [f]	Comment
$(1s^2 2s_{1/2} 5p_{3/2})_2 \rightarrow (1s^2 2s^2_{1/2})_0$	1	22.213	XIII-1	4	22.204	0.010	0.009	...	...	...	...	...
...	...	...	...	...	...	...	...	23.100	...	...	...	...
$(1s^2 2s_{1/2} 5d_{5/2})_4 \rightarrow (1s^2 2s_{1/2} 2p_{3/2})_2$	1	24.331	XIII-2	8	24.415	0.008	-0.084	...	...	...	...	...
$(1s^2 2s_{1/2} 4p_{3/2})_2 \rightarrow (1s^2 2s^2_{1/2})_0$	4	24.589	XIII-3	13	24.590	0.003	-0.001	...	...	...	...	...
...	...	...	...	...	...	...	...	26.400	...	...	...	...
$(1s^2 2s_{1/2} 4d_{5/2})_4 \rightarrow (1s^2 2s_{1/2} 2p_{3/2})_2$	3	27.089	XIII-4	3	26.973	0.005	0.116	...	...	...	...	...
$(1s^2 2s_{1/2} 4s_{1/2})_0 \rightarrow (1s^2 2s_{1/2} 2p_{3/2})_2$	1	27.514	XIII-5	3	27.405	0.005	0.109	...	...	...	...	...
$(1s^2 2s_{1/2} 3p_{3/2})_2 \rightarrow (1s^2 2s^2_{1/2})_0$	4	32.201	XIII-6	20 [g]	32.238	0.003	-0.037	32.236	-0.002	32.1910	-0.047	blend of 2 predicted lines
$(1s^2 2s_{1/2} 3p_{1/2})_2 \rightarrow (1s^2 2s^2_{1/2})_0$	19	32.247	XIII-6	20 [g]	32.238	0.003	0.009	32.236	-0.002	32.2420	0.004	blend of 2 predicted lines
$(1s^2 2s_{1/2} 3d_{3/2})_4 \rightarrow (1s^2 2s_{1/2} 2p_{1/2})_2$	1	33.855	XIII-7	5	33.821	0.002	0.034	33.843	0.023	...	...	shoulder of XIII-8
$(1s^2 2s_{1/2} 3d_{5/2})_6 \rightarrow (1s^2 2s_{1/2} 2p_{3/2})_4$	2	33.955	XIII-8	13	33.942	0.003	0.013	33.945	0.003	33.9510	0.009	...
$(1s^2 2s_{1/2} 3d_{5/2})_4 \rightarrow (1s^2 2s_{1/2} 2p_{3/2})_2$	20	35.849	XIII-9	20	35.669	0.003	0.180	35.614	-0.055	35.6670	-0.002	...
...	...	...	XIII-9	20	35.669	0.003	0.180	35.665	-0.004	...	...	...
$(1s^2 2s_{1/2} 3d_{5/2})_2 \rightarrow (1s^2 2p^2_{3/2})_0$	2	36.698	...	...	...	...	...	...	...	...	...	blend w/ XII
$(1s^2 2p_{3/2} 3s_{1/2})_2 \rightarrow (1s^2 2p_{1/2} 2p_{3/2})_4$	1	36.923	...	...	...	...	...	...	...	...	...	...
$(1s^2 2s_{1/2} 3s_{1/2})_0 \rightarrow (1s^2 2s_{1/2} 2p_{3/2})_2$	10	37.844	XIII-10	19	37.609	0.003	0.235	37.600	-0.009	37.598	-0.011	blend w/ several
$(1s^2 2s_{1/2} 3p_{3/2})_4 \rightarrow (1s^2 2p^2_{1/2})_4$	1	38.943	...	...	...	...	...	...	...	...	...	blend w/ XII-8

[a] Relative to strongest peak, scale 1–20

[b] $\lambda_{HULLAC} - \lambda_{EBIT}$

[c] Kaastra & Mewe 1993; Mewe, Kaastra, & Liedahl 1995

[d] $\lambda_{MEKAL} - \lambda_{EBIT}$

[e] Dere et al. 1997, 2001

[f] $\lambda_{CHIANTI} - \lambda_{EBIT}$

[g] Combined intensity of blended feature

Table 8. Summary of S XIV emission data.

HULLAC Transition	HULLAC Intensity [a]	HULLAC λ (Å)	Feature	Measured Intensity [a]	Measured λ (Å)	St. Error	Δλ [b]	MEKAL λ (Å) [c]	Δλ [d]	CHIANTI λ (Å) [e]	Δλ [f]	Comment
...	...	...	...	...	...	...	...	21.000	...	...	...	...
$(1s^2 5d_{5/2})_{5/2} \rightarrow (1s^2 2p_{3/2})_{3/2}$	1	21.740	XIV-1	13	21.613	0.008	0.127	...	...	...	...	...
$(1s^2 4p_{3/2})_{3/2} \rightarrow (1s^2 2s_{1/2})_{1/2}$	3	23.010	XIV-2	17 [g]	23.020	0.007	-0.010	23.050	0.030	23.005	-0.015	blend of 2 predicted lines
$(1s^2 4p_{1/2})_{1/2} \rightarrow (1s^2 2s_{1/2})_{1/2}$	1	23.020	XIV-2	17 [g]	23.020	0.007	0.000	23.050	0.030	23.015	-0.005	blend of 2 predicted lines
$(1s^2 4d_{3/2})_{3/2} \rightarrow (1s^2 2p_{1/2})_{1/2}$	1	24.214	XIV-3	20 [g]	24.257	0.006	-0.043	24.200	-0.057	24.200	-0.057	blend of 2 predicted lines
$(1s^2 4d_{5/2})_{5/2} \rightarrow (1s^2 2p_{3/2})_{3/2}$	2	24.298	XIV-3	20 [g]	24.257	0.006	0.041	24.200	-0.057	24.285	0.028	blend of 2 predicted lines
...	...	...	...	...	24.415	0.008	...	...	...	24.418	0.003	...
$1s^2 4s_{1/2})_{1/2} \rightarrow (1s^2 2p_{3/2})_{3/2}$	1	24.521	...	...	24.415	0.008	0.106	24.500	0.085	24.508	0.093	blend w/ XIII-2
$(1s^2 3p_{3/2})_{3/2} \rightarrow (1s^2 2s_{1/2})_{1/2}$	20	30.436	XIV-4	18 [g]	30.447	0.005	-0.011	30.423	-0.024	30.427	-0.020	blend of 2 predicted lines
$(1s^2 3p_{1/2})_{1/2} \rightarrow (1s^2 2s_{1/2})_{1/2}$	10	30.477	XIV-4	18 [g]	30.447	0.005	0.030	30.423	-0.024	30.469	0.022	blend of 2 predicted lines
$(1s^2 3d_{3/2})_{3/2} \rightarrow (1s^2 2p_{1/2})_{1/2}$	9	32.437	XIV-5	11	32.415	0.006	0.022	32.430	0.015	32.416	0.001	...
$1s^2 3d_{5/2})_{5/2} \rightarrow (1s^2 2p_{3/2})_{3/2}$	17	32.58	XIV-6	15 [g]	32.559	0.003	0.021	32.554	-0.005	32.560	0.001	blend of 2 predicted lines
$1s^2 3d_{3/2})_{3/2} \rightarrow (1s^2 2p_{3/2})_{3/2}$	2	32.594	XIV-6	15 [g]	32.559	0.003	0.035	32.554	-0.005	32.575	0.016	blend of 2 predicted lines
$1s^2 3s_{1/2})_{1/2} \rightarrow (1s^2 2p_{1/2})_{1/2}$	5	33.404	XIV-7	2	33.383	0.008	0.021	33.259	-0.124	33.381	-0.002	...
$1s^2 3s_{1/2})_{1/2} \rightarrow (1s^2 2p_{3/2})_{3/2}$	9	33.572	XIV-8	4	33.560	0.006	0.012	33.425	-0.135	33.549	-0.011	...

[a] Relative to strongest peak, scale 1–20

[b] $\lambda_{HULLAC} - \lambda_{EBIT}$

[c] Kaastra & Mewe 1993; Mewe, Kaastra, & Liedahl 1995

[d] $\lambda_{MEKAL} - \lambda_{EBIT}$

[e] Dere et al. 1997, 2001

[f] $\lambda_{CHIANTI} - \lambda_{EBIT}$

[g] Combined intensity of blended feature

Table 9. Comparison of EBIT-II data with major databases. Columns list the number of lines for each charge state. Data are for the region 20–75 Å.

Charge State	EBIT-II	MEKAL[a]	CHIANTI[b]
S VII	10	9	0
S VIII	25	6	0
S IX	22	3	0
S X	29	5	1
S XI	14	4	0
S XII	9	3	4
S XIII	10	8	5
S XIV	8	9	13

[a]Kaastra & Mewe 1993; Mewe, Kaastra, & Liedahl 1995

[b]Dere et al. 1997, 2001

University of California
Lawrence Livermore National Laboratory
Technical Information Department
Livermore, CA 94551